

Real-time Modeling of Battery Pack Temperature for Thermal Limit Prevention in Electric Race Vehicles

An Undergraduate Honors Thesis

Submitted to the Department of Mechanical Engineering

The Ohio State University

In Partial Fulfillment of the Requirements

For Graduation with Honors Research Distinction in Mechanical Engineering

Polina Brodsky

Spring, 2016

Dr. Marcello Canova, Advisor

Abstract

As the automotive industry moves towards reducing CO₂ emissions, battery powered electric vehicles are becoming a commercial reality. Though Lithium ion battery technology has significantly improved with recent research and development efforts, batteries still suffer from fundamental thermal limits that can decrease vehicle longevity, durability, and safety. Currently, methods exist to model temperature behavior of individual cells and heavy computational resources can be used to predict battery pack temperatures.

This study develops a computationally fast simulation tool that provides real-time prediction of the temperature of a battery pack. Unlike the methods currently available, this simulation tool is based on an accurate and robust electrochemical-thermal model for a Lithium ion battery pack that predicts the temperature distribution across the cells during current cycling operations with real-time computation capabilities. Starting from a pre-existing electrochemical-thermal model developed for individual cells, a predictive battery temperature model characterizing thermal losses and heat transfer parameters of full battery packs was created, verified, and tuned. The properties of the battery pack, such as battery chemistry, spatial cell arrangement, and electrical layout, can then be altered in the model to perform design experiments comparing differing pack parameters. The developed model is a useful tool to study the dynamic behavior of any vehicular battery pack, to inform pack cooling design, and to be used in advanced temperature management systems to control and predict battery temperature.

Acknowledgements

I would like to thank Dr. Marcello Canova for advising me on this research thesis. His expertise in batteries and dynamic system modeling were integral to this project, and he helped guide me through the entire research process. The encouragement and advice I received from Dr. Canova was indispensable for the successful completion of this project.

I would also like to thank Guodong Fan for his guidance in the battery modeling process. His help with the electrochemical modeling and advice on thermal modeling parameters was appreciated and valuable for this project.

Additionally, I would like to thank Buckeye Current for teaching me more than I ever thought I could learn about battery design and providing me with countless opportunities to grow as an engineer.

Finally, I would like to thank the Ohio State University Center for Automotive Research for allowing me to do my research at its facilities.

Table of Contents

Abstract	2
Acknowledgements.....	3
List of Figures	5
List of Tables	7
Chapter 1: Introduction	8
Buckeye Current: Electric Racing at Ohio State	8
Motivations for Thermal Modeling of Lithium Ion Packs.....	12
Research Objectives.....	14
Chapter 2: Background.....	16
Basic operating principles of Li-Ion cells.....	16
Overview of battery packs and design principles.....	17
Chapter 3: Description of Experimental Setup	20
Single cell discharge.....	20
Test pack design	20
Test pack discharge.....	22
Chapter 4: Electro-thermal model development	26
Electrochemical Model Background and Theory.....	26
Single Cell Thermal Model.....	31
Full Pack Thermal Model	35
Chapter 5: Case Studies.....	42
Effects of cell spacing	42
Effects of Air Speeds	43
Effects of Cell Chemistry	45
Parallel Configuration	46
Chapter 6: Conclusion/ Recommendation for future work	47
References	50
Appendix A: Parameter Values Used in Thermal Models	52

List of Figures

Figure 1: RW-3 electric motorcycle.....	9
Figure 2: Schematic of RW-3 powertrain.	10
Figure 3: RW-3 battery pack.....	11
Figure 4: Battery pack position on RW-3.	11
Figure 5: Battery thermal limit at PPIHC 2015.	13
Figure 6: Lithium ion battery schematic [2].	16
Figure 7: Prototype pack layout.	21
Figure 8: Thermistor location and measurements in prototype pack.	22
Figure 9: Wind tunnel air flow direction.....	23
Figure 10: Row 5-6 air temperatures in test pack	24
Figure 11: Row 2-3 air temperatures in test pack	24
Figure 12: Bus bar temperatures in test pack	25
Figure 13: Methodology for modeling pack thermal performance.	26
Figure 14: Schematic of reduced order electrochemical model. [4]	27
Figure 15: Block diagram of reduced-order battery electrochemical model. [4]	28
Figure 16: OCP profiles for NCA electrochemical model.	29
Figure 17: Model comparison to 0.1C discharge data.	30
Figure 18: Model comparison to 0.1C discharge data.	30
Figure 19: Model comparison to 0.1C discharge data.	31
Figure 20: Single pack discharge model vs experimental data.....	34
Figure 21: Schematic of full pack thermal model.	35
Figure 22: Sources of heat transfer in full pack thermal model.....	36
Figure 23: Full pack experimental data vs model at 18 m/s inlet air speed.....	40
Figure 24: Predicted cell temperatures in prototype pack.....	41
Figure 25: Model GUI.	41
Figure 26: Temperature profiles at different cell spacing.....	42
Figure 27: Spacing effect on cell temperature.	43
Figure 28 Temperature profiles at different air inlet velocities.	44

Figure 29: Air velocity effect on cell temperature	45
Figure 30: A123 vs Samsung predicted thermal performance.	45
Figure 31: Parallel string configuration effect on cell temperature.	47
Figure 32: PPIHC 2016 battery pack placement in vehicle.	49
Figure 33: RW-3x battery pack isometric view.....	49

List of Tables

Table 1: Comparison of Samsung and A123 power and energy densities.	46
Table 2: Parameters used in single cell thermal model (Samsung 25R)	52
Table 3: Parameters used in full pack thermal model of test pack.....	53

Chapter 1: Introduction

Buckeye Current: Electric Racing at Ohio State

This research project is inspired by Buckeye Current, the electric motorcycle race team at The Ohio State University. Buckeye Current is a student-led motorsports team that designs, builds and races electric motorcycles in international competition. Since its founding in 2011, the team has achieved two Isle of Man (IOM) TT Zero third place finishes (2013, 2014), an East Coast Timing Association (ECTA) speed record (2011, 2012) and a 2nd place electric class finish at Pikes Peak International Hill Climb (PPIHC) (2015). These achievements have earned Buckeye Current the title of being the world's fastest collegiate electric motorcycle.

Buckeye Current is primarily composed of undergraduate engineering students. One of the main focuses of the team lies in technical advancement of electric vehicle technology. Though the team's members are young, Buckeye Current prides itself in competing against not just collegiate race teams, but also professional race teams. Aside from technical achievements, the team's other primary goal is the education of members and the community at large. By involving undergraduate engineers in the team and training them to work on the vehicle at such a detailed level of design, the team cultivates engineering talent and allows members to develop design and project management skills.

Electric racing pushes the limits of electric vehicle technology and promotes zero-emission vehicles by showcasing the ability of electric power in some of the world's fastest driving machines. The development of electric race vehicles is integral to the push towards CO₂ emission reduction, and the work Buckeye Current does advances the state of the art in electric vehicle technology.

Description of the RW-3 Motorcycle

In 2014, Buckeye Current designed a motorcycle, RW-3, to compete at the 2015 Pikes Peak International Hill Climb. PPIHC is a 12.41 mile course with a 156 turns and a 5000 foot elevation gain that races up one of Colorado's tallest mountains to a finish line over 14,000 feet above sea level [1].

The design of RW-3 is based on the frame of a modified 2008 Honda CBR1000RR. The electric powertrain of the motorcycle was designed and integrated entirely by Ohio State students, and includes a custom built battery pack with custom-made Battery Management System, an Emrax 268MV permanent magnet axial flux AC electric motor, a Tritium Wavesculptor 200 motor controller, and a custom made data logging system with over 35 sensors on the vehicle. Figure 1 illustrates the RW-3 motorcycle while Figure 2 presents a basic schematic of the components of the powertrain.



Figure 1: RW-3 electric motorcycle.

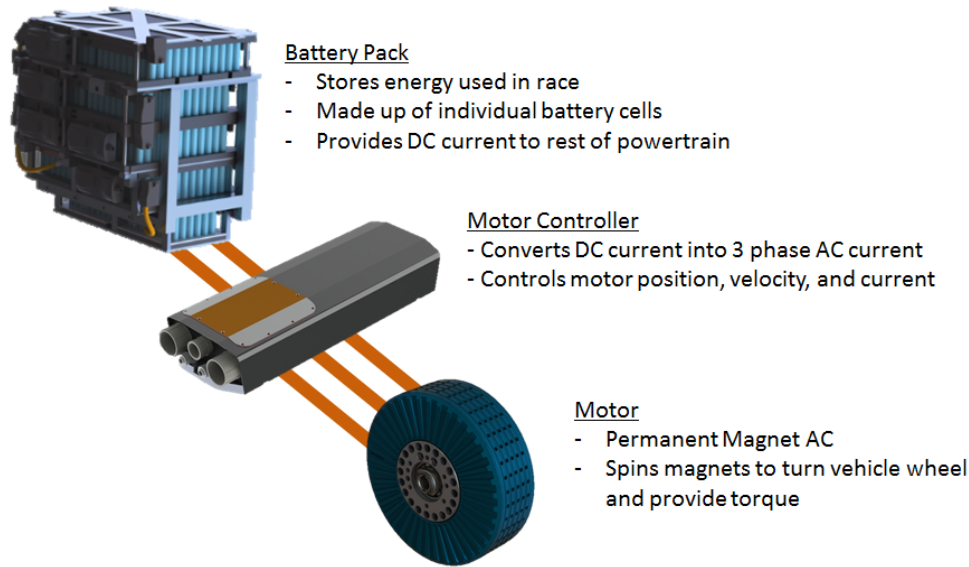


Figure 2: Schematic of RW-3 powertrain.

The motorcycle has an air-cooled, 450V, 8.7kWh Li-ion battery pack (made up of 972 individual cylindrical Samsung 25R battery cells) with a peak power of over 120kW. The pack is configured at 108s9p, with 9 cells in parallel and 108 series strings. There are 5 layers of cells aligned in a rectangular formation in the pack. The top 4 layers contain 24 series strings (216 cells per layer, 864 cells total) while the bottom layer is smaller, and only has 12 series strings (108 cells). The cells are connected together using nickel bus bars, and copper cables make the connection between layers in the pack and from the pack to the rest of the vehicle's powertrain.

The battery pack design was extremely constrained by the volume available in RW-3. Due to the need for small frontal area to reduce drag and large ground and lean angle clearances, the pack was designed to be compact and fit beneath the main frame of the motorcycle. As weight is also a concern in racing applications, the battery pack was designed to be as light as possible by using HDPE plastic materials to contain and isolate the cells. The final weight of the battery pack was approximately 50 kg. Figure 3 shows an isometric view of the battery pack, and Figure 4 illustrates its position in RW-3.



Figure 3: RW-3 battery pack.

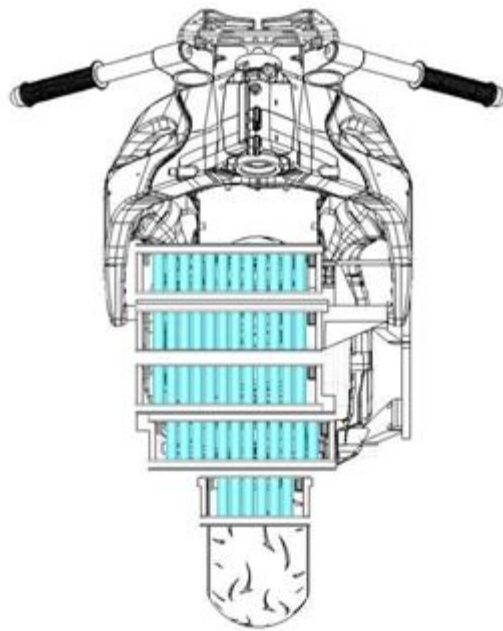


Figure 4: Battery pack position on RW-3.

Motivations for Thermal Modeling of Lithium Ion Packs

On June 28, 2015 Buckeye Current raced at PPIHC to a second place finish in its all-electric class, with a time of 11:12.756. Though this debut performance was respectable, the team's vehicle suffered from thermal limits in its battery pack that greatly hindered the performance of its motorcycle on the course.

Telemetry data collected during the race showed that the high currents drawn during the race generated significant heat rejection, which caused the pack temperature to rise rapidly in a due to packaging and cooling limitations. To prevent damage to the battery cells, the Battery Management System (BMS) includes a power limit on the vehicle that activates after the highest measured cell temperature in the pack exceeds 55°C. At the 2015 PPIHC event, this temperature limit was achieved just after the 6th minute of the race, resulting in a power limit for the last 5 minutes of its run [Figure 5].

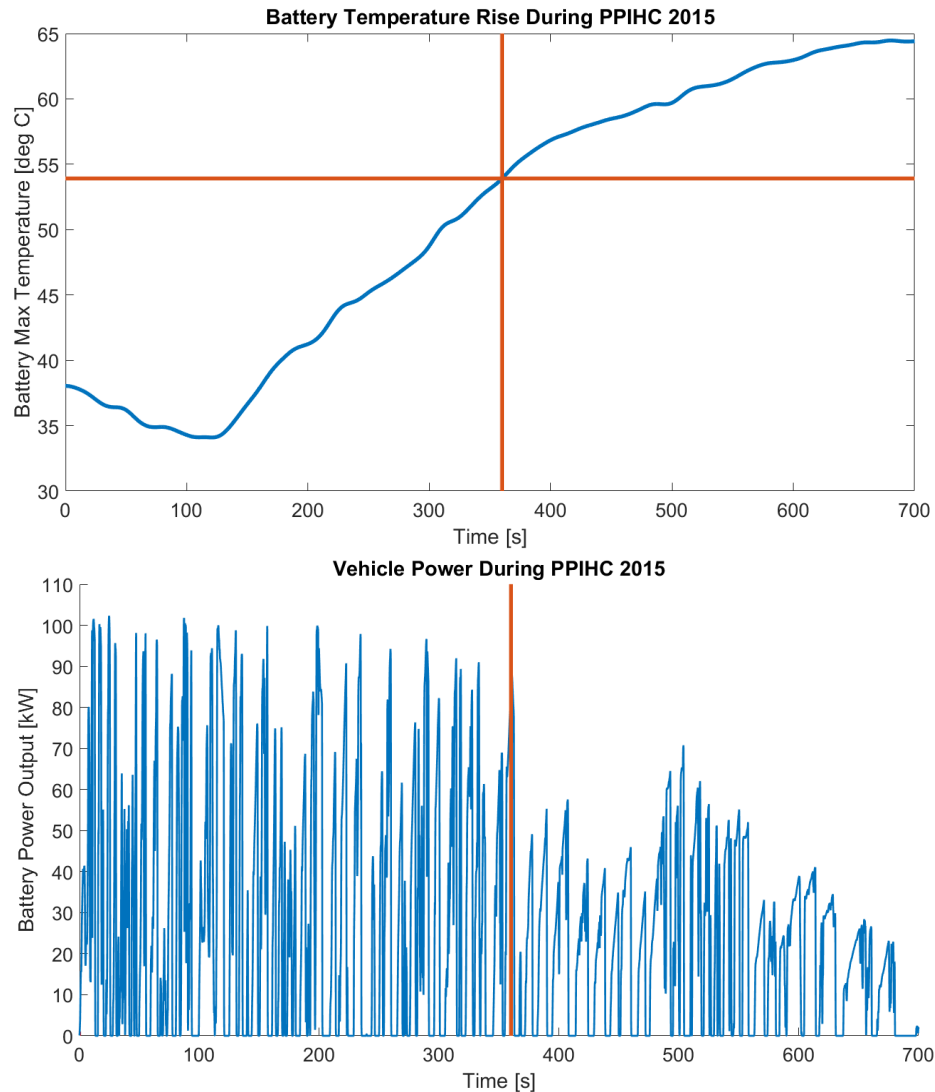


Figure 5: Battery thermal limit at PPIHC 2015.

After the race data were analyzed, it was clear that, to prevent future performance limitations, design optimization on the team's battery pack is required. The battery pack for the team must be redesigned with a short development cycle and tight budget, however, and this requires faster and more cost-effective approaches than building prototype packs and testing them. Physics based models – derived from first from principles and verified experimentally – are an effective tool to conduct virtual pack design. For this reason, a robust battery pack thermal model would be needed to provide detailed information on

the cell temperature distribution within the pack during race conditions. Creating a comprehensive, accurate thermal model to predict cell temperatures for Buckeye Current's race vehicle would allow for the team to better design its battery configuration, geometry, and cooling to prevent cell overheating during the race. Furthermore, predicting if battery temperature will cause power limiting would allow the team to calculate race performance by understanding where vehicle power limits will occur on the course and how they will affect overall vehicle speeds.

Similar issues, though to a lesser extent, can be found in electric vehicles and hybrid electric vehicles in production applications. Although average pack temperature is regulated, thermal gradients still occur within the pack cells. Poor cooling and thermal gradients in battery packs expose cells to high temperatures, which accelerates degradation, reduces cell life, and can potentially lead to catastrophic failures. As cells degrade faster, maximum temperatures of the cells are approached more quickly. This causes vehicle performance to be reduced sooner, since motor torque is derated when the highest measured cell temperature exceeds a threshold. The compromise of vehicle safety and performance that occurs when cells are exposed to high temperatures is an important reason for the investigation of better thermal management in electric vehicle battery packs.

A compelling need for developing predictive and robust models that can simplify estimator design and tuning processes exists for electric vehicles. These models would improve the effectiveness of model-based thermal monitoring and would support the design of thermal management strategies for enhanced battery performance and extended pack life.

Research Objectives

The objective of this research is to develop a framework to inform battery pack thermal analysis and design based on the use of physics-based modeling and simulation tools. Such tools would assist the

designers of the energy storage system in making choices for the battery pack of the electric motorcycle, for instance by evaluating the impact of different battery configurations on the temperature distribution and the possible onset of thermal limits when the battery pack is in use.

Furthermore, this method would allow for real-time on board temperature prediction for battery packs. By modeling the electrochemical and thermal behavior of each individual cell within the pack, the model would provide more information than simply averaging the pack temperature but be less computationally intense than performing full Computational Fluid Dynamics (CFD) analysis on a battery pack. A fast computation time could allow the model to be integrated into battery temperature control systems as a real-time monitoring algorithm which could in turn improve the performance of Battery Management Systems (BMS).

A model such as the one proposed in this work would become an asset in the development of future projects for Buckeye Current, in that it would allow the team to design battery packs with better cooling characteristics, and ultimately to further improve the performance and reliability of their electric race motorcycles. This model could also become useful in other electric race vehicles and consumer electric vehicles, in that it would allow for real-time temperature prediction and management of battery packs.

This work is structured as follows. First, a cell-level electrochemical model was adapted from prior work at OSU-CAR in order to predict battery voltage behavior with different discharge parameters. Then, a single cell thermal model was created, integrated with the electrochemical model and verified with cell discharge data. Next, a full pack thermal model was created and tuned to match experimental data collected on a prototype pack. Finally, the model was extended to allow the user to evaluate of the electrical and thermal performance of packs varying the battery chemistry, cell parameters, cell electrical connections and configuration within the pack, and cooling parameters.

Chapter 2: Background

Basic operating principles of Li-Ion cells

A lithium-ion battery is generally constituted by a pair of electrodes, where the positive electrode (cathode) is predominantly composed by a lithium metal oxide ($LiMO_x$) (where M stands for metal) on an aluminum foil, and the negative electrode (anode) is constituted by lithiated graphitic carbon sputtered over a copper foil. The metal oxide and lithiated carbon are the active materials of the electrodes. A microporous polymer separator film or gel-polymer is inserted between the electrodes to prevent short circuits. Finally, the electrodes and separator are flooded with an electrolyte solution, generally a Lithium salt in an organic solvent. The electrolyte solution enables lithium ions to move between the positive and negative electrodes during charge and discharge operations [2]. Figure 6 shows a schematic of representation of the basic operation of a lithium ion cell.

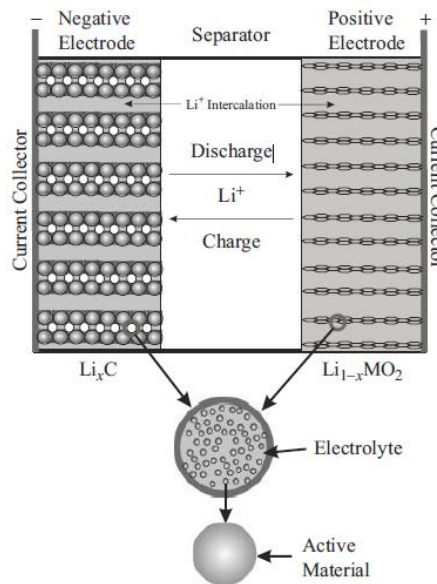
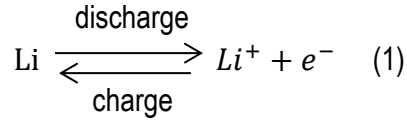
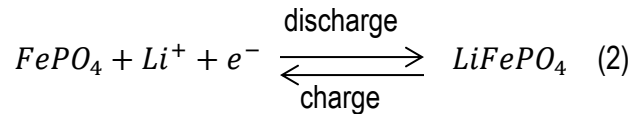


Figure 6: Lithium ion battery schematic [2].

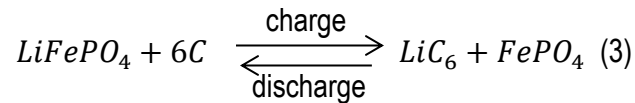
In a lithium-iron phosphate (LiFePO_4) battery, for example, the active material in the negative anode is oxidized during discharge, producing lithium ions that enter the electrolyte solution:



In this phase, the ions move through the separator under electrostatic forces and reach the cathode with the help of electrolyte to the positive electrode. Upon reaching the cathode, the lithium ions combine with the active material through a process known as intercalation, which can be modeled with the following reaction:



The complete reaction that describes the process in a $\text{LiFePO}_4/\text{LiC}$ cell results from combination of the two electrode reactions:



Overview of battery packs and design principles

In the design of battery systems for electric vehicles, there are many considerations that must be taken into account. It is well known that manufacturing a battery cell with enough energy and power density to meet the requirements of most electric vehicle powertrain systems is unfeasible for many reasons. In order to solve this, several cells must be used to compose a battery pack. Designing battery packs is a complex engineering problem that involves thermal management, monitoring and control, battery cell balancing, and

manufacturing. A well designed battery pack is thermally managed, structurally designed, electrically protected, and electronically controlled.

Before a battery pack can be designed, system level requirements for the vehicle must be determined. The total system energy, power, weight, and volume must be determined before battery pack design can begin. These factors are determined by drive cycle requirements, budget, vehicle size, and performance targets.

Once this requirement generation is complete, the cell chemistry must be chosen. This chemistry choice is driven primarily by the power and energy requirements of the full vehicle system. Generally in batteries, there is an inverse relationship between a cell's power density and energy density. A cell must be selected that meets the gravimetric and volumetric power and energy density requirements of the system such that enough power and energy can be packaged on board the vehicle in the allotted mass and volume for the battery system.

When designing a battery pack, the cell form factor is also an important consideration. Lithium-ion batteries can be produced in multiple sizes, such as cylindrical, pouch or prismatic cells. While each aspect and size has its own benefits and drawbacks, this study considers the use of cylindrical cells. Due to the small amount of available space and the complex geometry of a motorcycle frame, the Buckeye Current team has found that small-format cylindrical cells are the best option for packaging and integration.

After the cell chemistry is chosen, the electrical configuration, namely selecting the number of cells in series and parallel connection, must be optimized. Most vehicles have a voltage limit set by other powertrain component limits, safety concerns, or manufacturing limits. This determines the series configuration of the battery pack. The parallel configuration of the battery pack is determined by both the energy requirements of the vehicle system (which influence the range) and by the specific requirements of

the cells. Parallel arrangements are usually optimized to ensure that each cell does not draw more current than its continuous and peak C-rate capability, and so that the vehicle has enough energy on board to perform its intended function. Generally, higher voltage configurations tend to be more efficient than high current systems and need smaller conductor cross-sectional areas due to the lower current requirements, but can be more dangerous and difficult to package and assemble.

Once the pack electrical configuration is determined, bussing and packaging of the cells must be designed. Bussing of the cells can be accomplished in many ways. Mechanical joints such as bolts and rivets are common for pouch and prismatic cells, while welded bussing is commonly used for cylindrical cells. The shape, thickness, and material of the bus bar depends on multiple design factors including cell spacing within the battery pack, current requirements, mass restrictions, cell conductor materials, and manufacturing methods. Cells must also be packaged into the battery pack. In this case, the packaging design needs to accommodate environmental protection for the cells, mechanical fixturing, and electrical isolation. This also includes packaging of cooling systems for the cells. This can range from active cooling through liquid systems or air systems using fans, to passive systems using ducted airflow into the pack, phase-change materials, and heat sinks.

When designing battery packs, it is difficult to compare how cell packaging will affect system performance and how different cell choices (both in chemistry and form factor) will affect battery performance, hence many designers rely on previous experience. In addition, specifically with air cooled cylindrical cells, understanding the effect that cell spacing, cell arrangement, parallel configuration, cell chemistry, and cell size has on pack thermal performance is necessary for battery pack design. For this reason, a tool was developed to assist in the understanding of these parameters' effects on pack performance, so that pack design can be optimized to maximize cell performance and meet system requirements.

Chapter 3: Description of Experimental Setup

Single cell discharge

To accurately model the cell temperature behavior under different discharge conditions, an accurate representative model predicting the cell voltage under different loads is required. This model was created using data from single cell discharge tests.

To perform the testing, a single Samsung 25R cell was fitted with tabs and attached to a Maccor 4304 programmable load and supply system. This unit made it possible to run different discharge profiles on the cell and monitor its voltage and current under load.

Multiple tests were run on an individual cell. This included constant C-rate discharging cycles at 0.1C, 0.8C, 3C, and 5.2C. The cell voltage was monitored for the entire range of the State of Charge (SOC) of the cell.

Test pack design

To obtain data for a full battery pack, a small pack was manufactured and tested. The battery pack was made of an 8s3p configuration of 2.5 Ah NCA Samsung 25-R 18650 cells. The cells were housed in layers of HDPE plastic to fixture the cells and electrically isolate the bus bars. Nickel strips were spot welded to each cell to make electrical connections in the pack. A layout of the battery pack can be found in Figure 7.

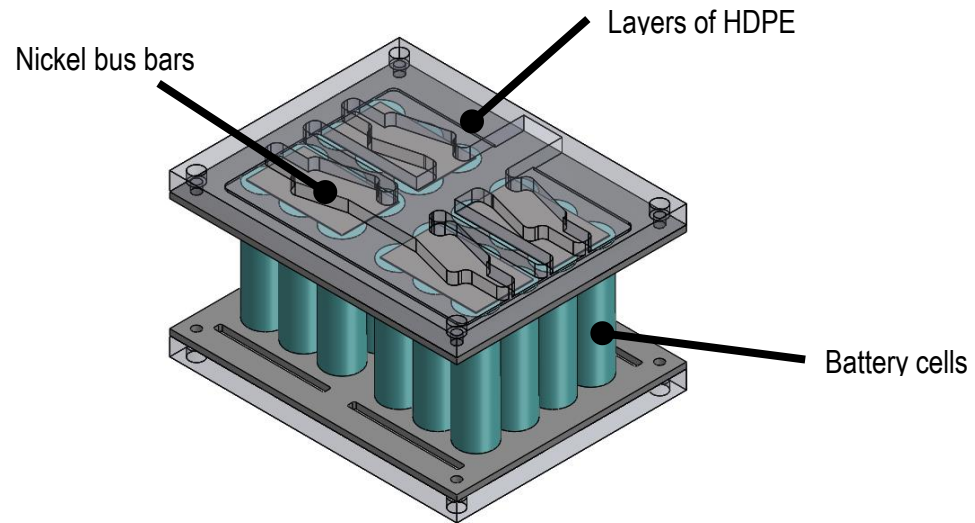


Figure 7: Prototype pack layout.

The prototype pack was instrumented with thermistors to measure temperatures of air between the gaps in the cells and the bus bars. The thermistors were instrumented as shown in Figure 8.

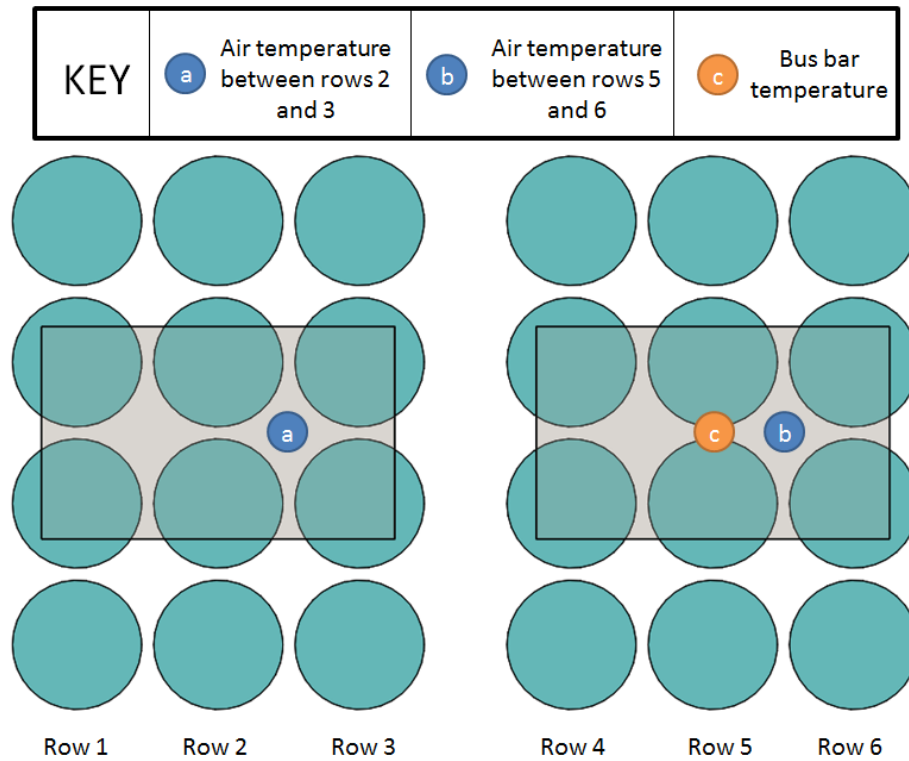


Figure 8: Thermistor location and measurements in prototype pack.

Test pack discharge

The prototype pack was placed in a wind tunnel and hooked up to an Amrel PLA programmable load. Figure 9 shows the orientation of the battery pack in the wind tunnel. It was discharged at a constant 5.2C as pack temperatures were measured. The wind tunnel was run at 4.5, 9, 18, and 27 m/s for each run.

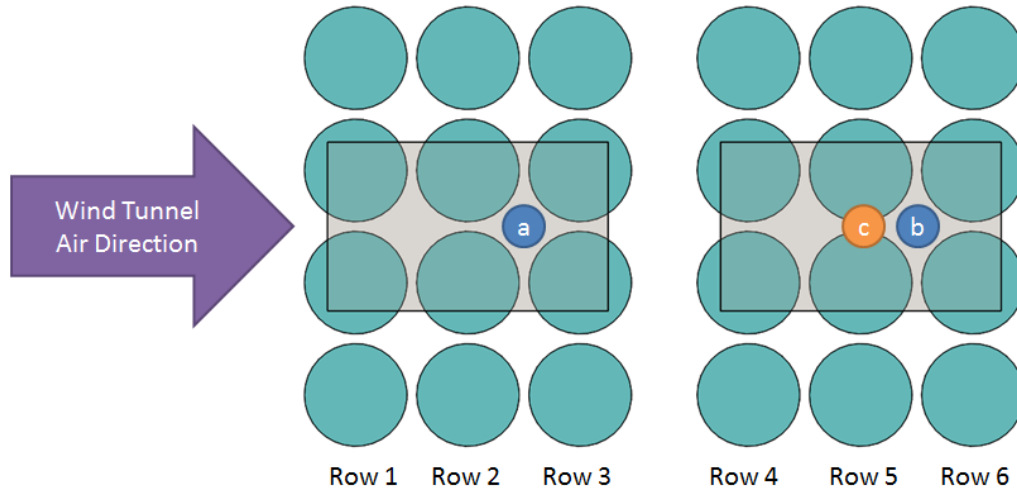


Figure 9: Wind tunnel air flow direction.

The results obtained from the experimental data are illustrated in Figure 10, Figure 11, and Figure 12.

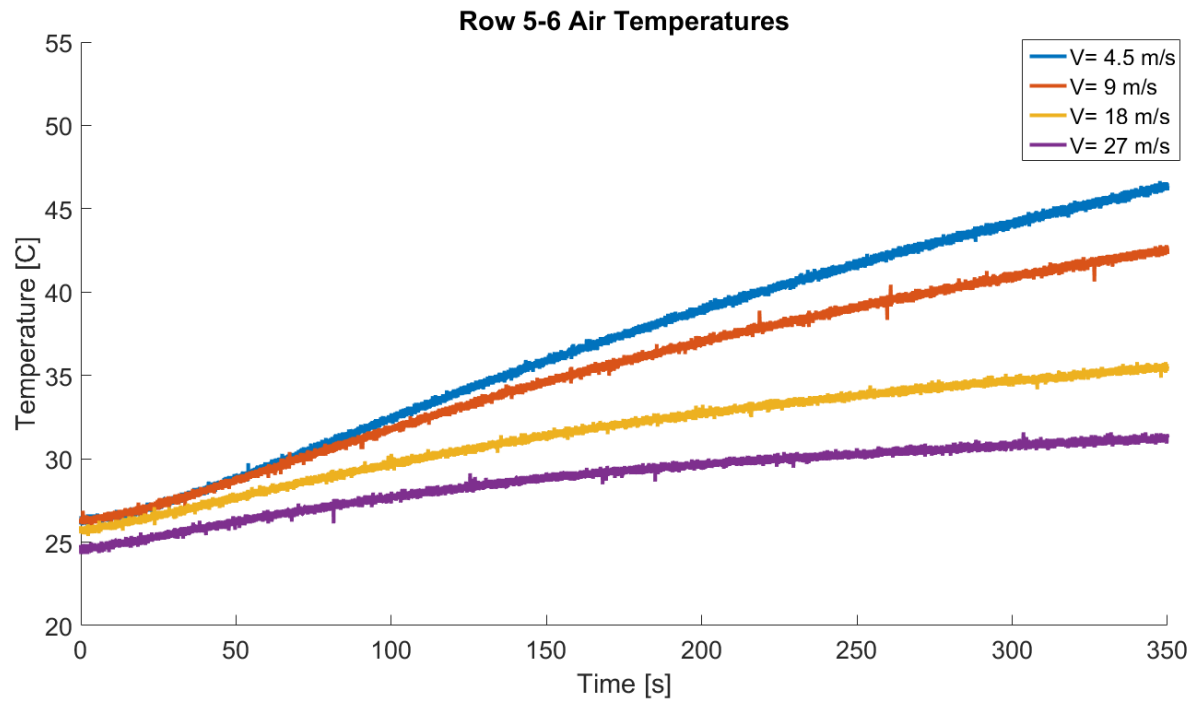


Figure 10: Row 5-6 air temperatures in test pack

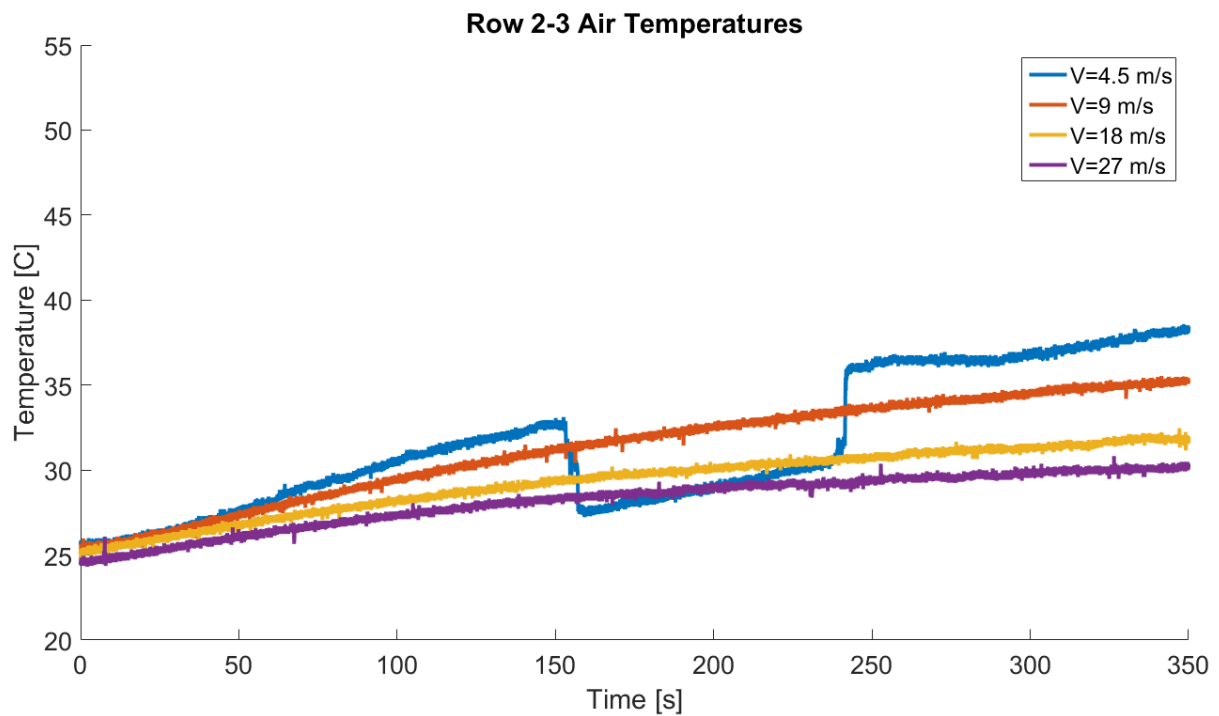


Figure 11: Row 2-3 air temperatures in test pack

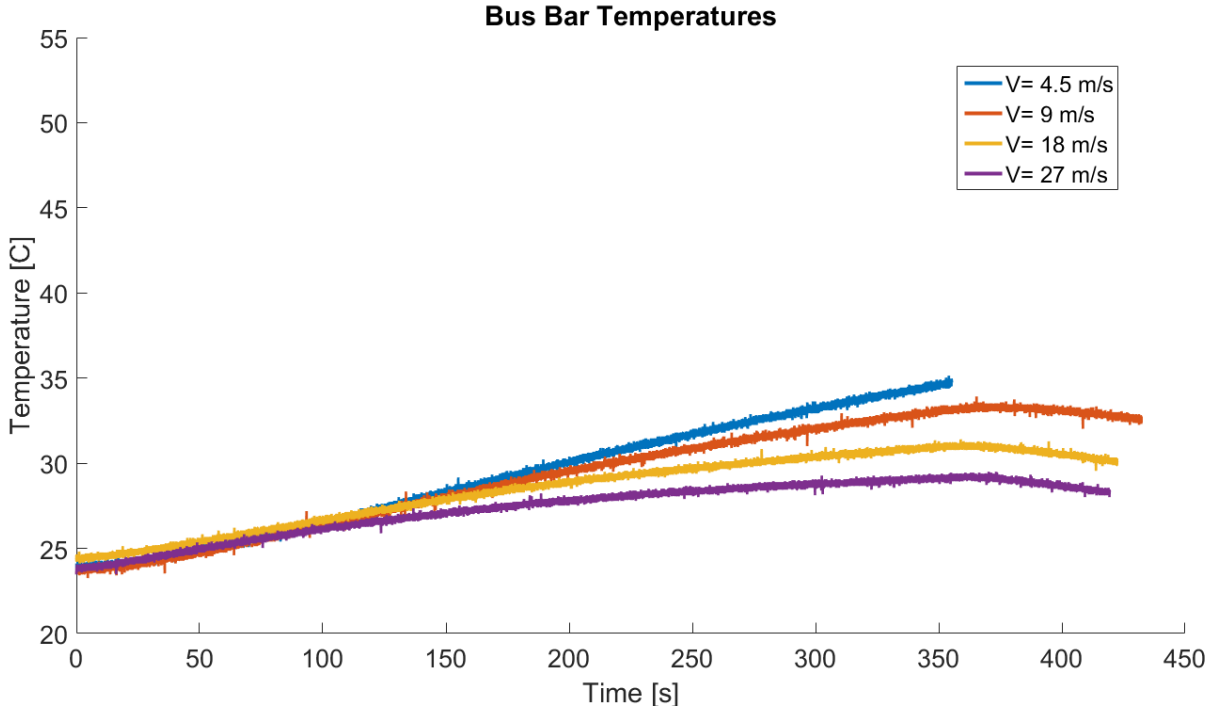


Figure 12: Bus bar temperatures in test pack

It can be noted that throughout each experiment the measured temperatures increased as inlet air velocity decreased. As expected, the measured temperature in row 5-6 is higher than those measured in row 2-3 due to row 2-3 being closer to the colder inlet air. The bus bar temperature at row 5-6 is low compared to the air temperatures in that region. This implies that there may be a high thermal resistance to the bus bar connection and not much heat transfer occurs to the bar.

Figure 11 suggests that there was a thermistor failure during testing for the 4.5 m/s air velocity. During the middle portion of the discharge the temperature drops severely. This data was salvaged for use by removing the offset that occurred in the middle of the testing.

Chapter 4: Electro-thermal model development

To model pack thermal behavior, a three-step approach was used, as illustrated in Figure 13. Initially, an electrochemical model was created to model cell voltage behavior. This was useful for characterizing the waste heat output of a cell during discharge. Next, a single cell thermal model was created. The single cell model validated individual cell thermal behavior. Finally, a full pack model was created to model the temperature behavior of arrays of multiple cells.

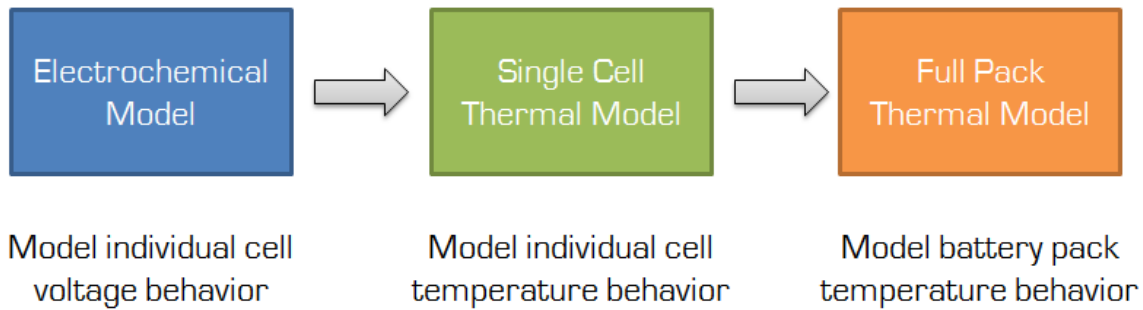


Figure 13: Methodology for modeling pack thermal performance.

Electrochemical Model Background and Theory

The reduced order electrochemical model used in this study stems from the single-particle model that has been previously implanted at CAR [3]. The model assumes that each electrode is represented by a single spherical particle and assumes that the total surface area of the particle is equal to that of the overall area of the active material in the porous electrode, as shown in Figure 14. The concentration overpotential in the model is modeled by solving a reduced-order liquid diffusion ordinary differential equation (ODE).

This leads to a diffusion based electrochemical model that accounts for the concentration dynamics in two of the electrodes and in the electrolyte. Then, a Pade approximation method is used to obtain a reduced-order model of cell behavior. A description of the governing equations and the Pade approximation can be found in [3].

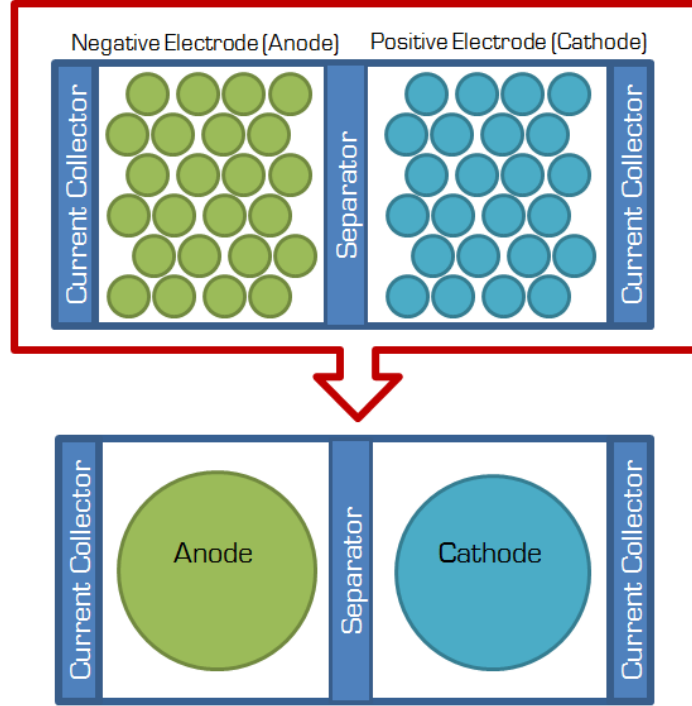


Figure 14: Schematic of reduced order electrochemical model. [4]

The block diagram for the resulting model can be seen in Figure 15. The cell output voltage can be obtained from the model as:

$$V_{cell} = \phi_p - \phi_e - \phi_n - IR_c = (U_p - \eta_p) - (U_n - \eta_n) - (\phi_L + IR_\Omega) - IR_c \quad (4)$$

Where U_p and U_n denote the open circuit voltage (OCV) of the positive and negative electrodes, respectively, η_p and η_n is the charge transfer overpotential, ϕ_L and IR_Ω represent the concentration

overpotential and the Ohmic potential drop in the liquid phase, and IR_c represents the Ohmic loss due to the current collectors.

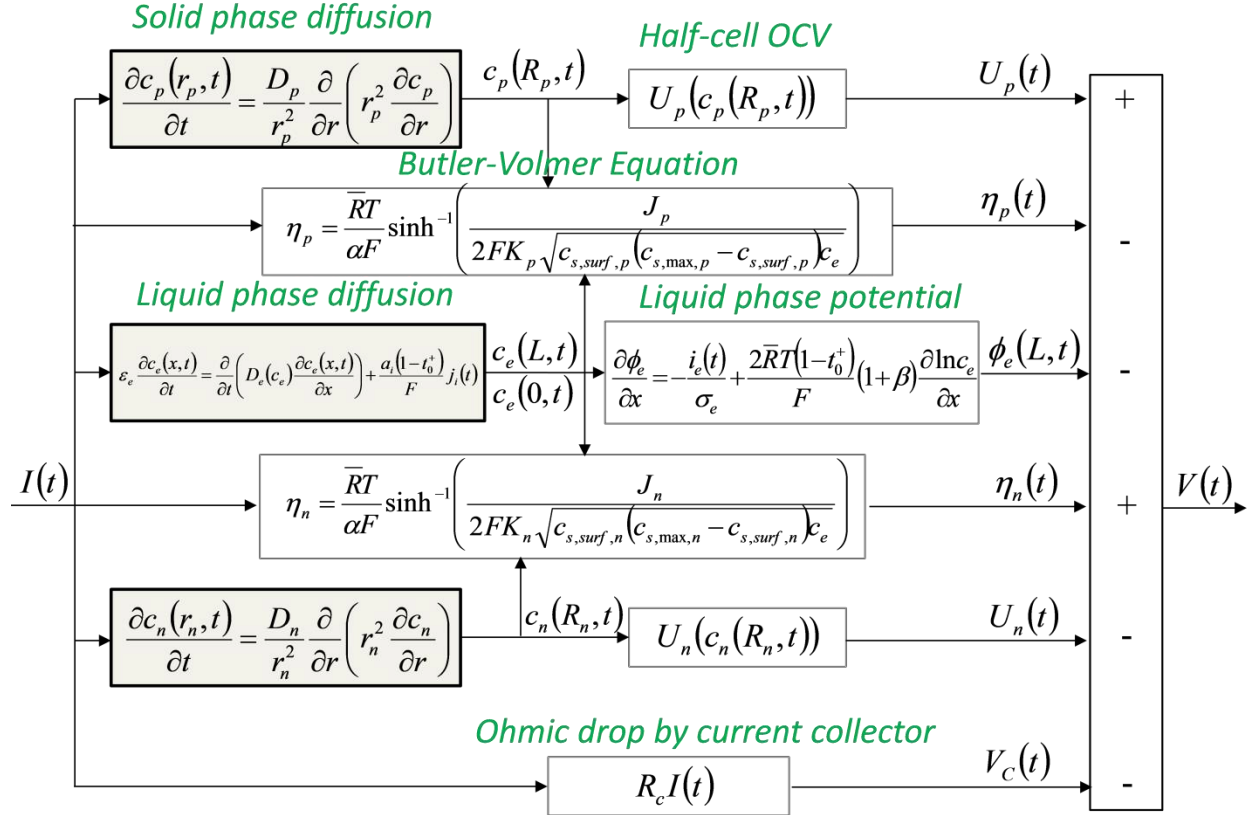


Figure 15: Block diagram of reduced-order battery electrochemical model. [4]

For this study, a comparison of A123's ANR26650 LiFePO₄ cell and Samsung's 25R 18650 NCA cell was performed. A preexisting model of the A123 cell parameters was used in the study. To create the Samsung 25R model, the data from the .1C, 0.8C, 3C, and 5.2C discharges was used to tune the cell voltage response.

To accomplish this, the positive electrode OCP was derived from the 0.1C discharge of the cell. Pre-existing profiles from the OCP of the electrolyte and negative electrode were subtracted from the total cell OCV to obtain the OCP of the NCA positive electrode (shown in Figure 16).

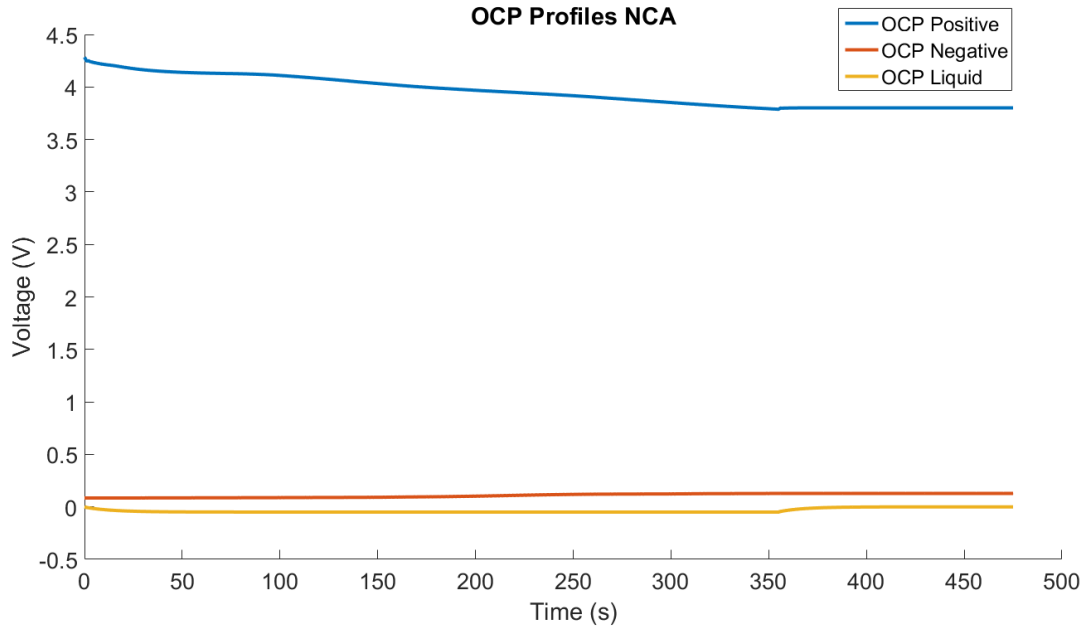


Figure 16: OCP profiles for NCA electrochemical model.

Once this curve was inserted into the model, the other diffusion constants, rate constants, and geometric parameters were tuned until the cell voltage prediction matched the experimental data. The 0.1C discharge of the cell was used in calibrating the discharge parameters, and the 0.8C, 3C, and 5.2C discharges were used to verify the calibration.

When the electrochemical model of the cells was completed and tuned, the model was able to accurately predict cell voltage across the entire SOC of the battery for different discharge profiles. Figure 17, Figure 18, and Figure 19 show the tuned model compared to the experimental discharge data at 0.1C, 0.8C, and 5.2C discharges of the Samsung 25R cell.

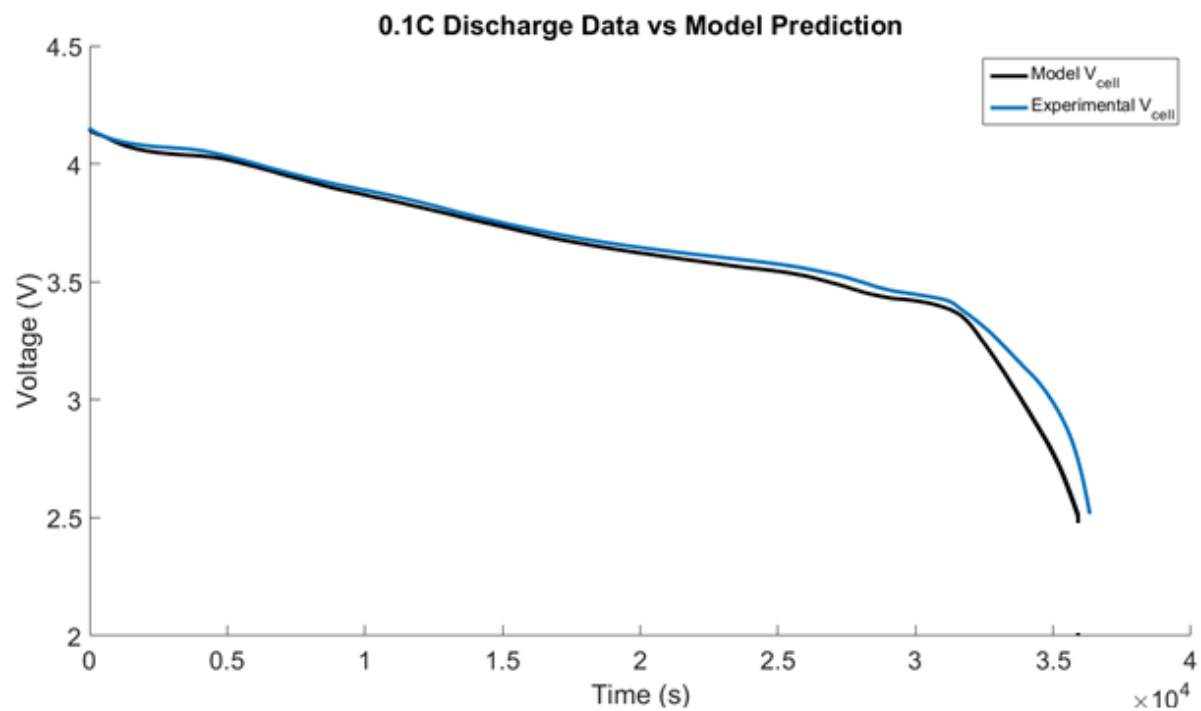


Figure 17: Model comparison to 0.1C discharge data.

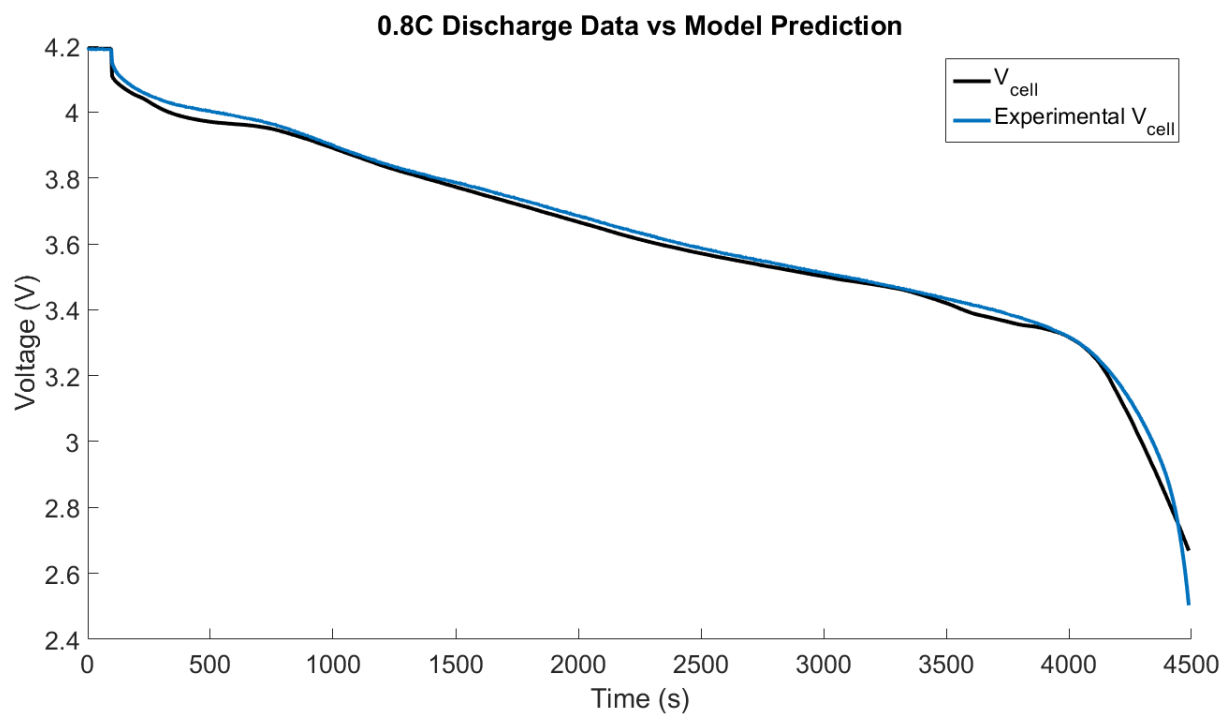


Figure 18: Model comparison to 0.1C discharge data.

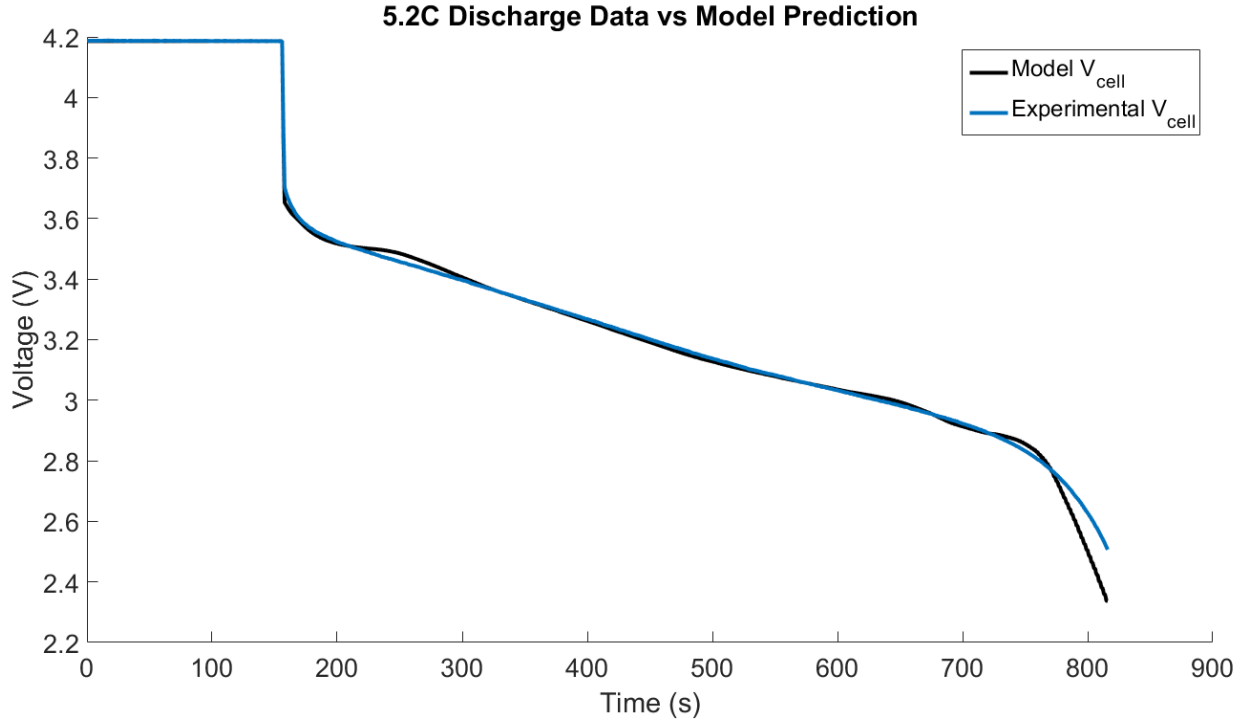


Figure 19: Model comparison to 0.1C discharge data.

Single Cell Thermal Model

Once the predictive cell voltage model was created, tuned and verified, this model was used to predict the heat output of the cell during its discharge:

$$q_{in} = I(V_{OC} - V) + q_{rev} \quad (5)$$

where q_{in} is the overall heat generation rate caused by the irreversibilities occurring within the cell (which includes Ohmic losses, activation losses and concentration losses, as indicated in Eq. (4)), I is the current draw, V_{OC} is the cell's open circuit voltage, and V is the cell's voltage and q_{rev} is the reversible heat loss in the cell, modeled by:

$$q_{rev} = IT \frac{\partial U}{\partial T} \quad (6)$$

In general, the reversible heat q_{rev} is small for high discharge rate conditions [6] [7] [8]. Since this study mainly dealt with experimental data above 5C discharges, it can be assumed that q_{rev} is negligible in the heat generation model.

This heat generated within the cell was then used as the input to a lumped thermal mass model of a single cell, based upon a simple energy balance:

$$q_{st} = c * q_{in} - q_{conv} - q_{rad} \quad (7)$$

where q_{st} is the heat energy stored in the cell, q_{conv} is the heat dissipated at the cell surface through convective heat transfer and q_{rad} is the radiative heat loss. c represents the percentage of the heat generated within the cell that is not dissipated through the tabs of the cell.

It can be noted that in the experimental discharge of the single cell, the battery was wedged between two large copper electrodes. When a cell is being connected to other cells within a pack or to a programmable load, a percentage of the thermal energy generated within the cell is extracted through the connection between its current collectors and the connectors at its positive and negative terminals. Because such a large heat sink was fixed to the electrodes in this experiment, a large portion of the heat was dissipated into the copper conductors. This was accounted for in the model by reducing the heat input into the cell with the constant c , which - when tuned to experimental data - was found to be 0.6.

The convective heat transfer from the cell was modeled using the expression:

$$q_{conv} = h_{conv}A(T_{cell} - T_{air}) \quad (8)$$

where h_{conv} is the convective heat transfer coefficient, A is the cell's surface area, T_{cell} is the temperature of the cell, and T_{air} is the ambient temperature of the air around the cell.

To calculate h_{conv} , a model for a horizontal cylinder with natural convection was used. The single cell discharge testing was done with the cell in a horizontal position with no cross-flow of air, so this was an accurate representation of the cell discharge. The coefficient h_{conv} was calculated using the following equation:

$$h_{conv} = a \frac{(Nu)(k)}{D} \quad (9)$$

where Nu is the Nusselt number, k is the thermal conductivity of air, D the cell's diameter, and a is a constant that was tuned to match the measured temperature of the cell measured in the single cell discharge. The Nusselt number was calculated using the correlation for natural convection [5]:

$$Nu = \left[\frac{0.60 + (0.387 Ra^{\frac{1}{4}})}{\left[1 + \left(\frac{0.559}{Pr} \right)^{\frac{9}{16}} \right]^{\frac{8}{27}}} \right]^2 \quad (10)$$

where Pr is the Prandtl number of air and Ra is the Raleigh number, defined as:

$$Ra = \frac{g B \rho^2 C_p (T_{cell} - T_{air}) D^3}{k \nu} \quad (11)$$

where ρ is the density of air, B is the coefficient of thermal expansion of air, C_p is the air specific heat, and ν is the air dynamic viscosity.

Radiative heat loss was found using:

$$q_{rad} = e \sigma A (T_{cell}^4 - T_{air}^4) \quad (12)$$

where e is the emissivity of the battery cell and σ is the Stephan-Boltzman constant. The emissivity of the cell was tuned to match the single cell discharge test profile.

For the single cell discharge, correlation was achieved to the experimental data after tuning the cell model to the discharge portion (0-800 seconds) of the experiment. The emissivity of the cell and the heat transfer coefficient were tuned with multipliers to minimize quadratic error on temperature. It can be noted from Figure 20 that the model predicts both discharge (between 0 and 800 seconds) as well as cool-down (after 800 seconds) when the cell is no longer drawing any current.

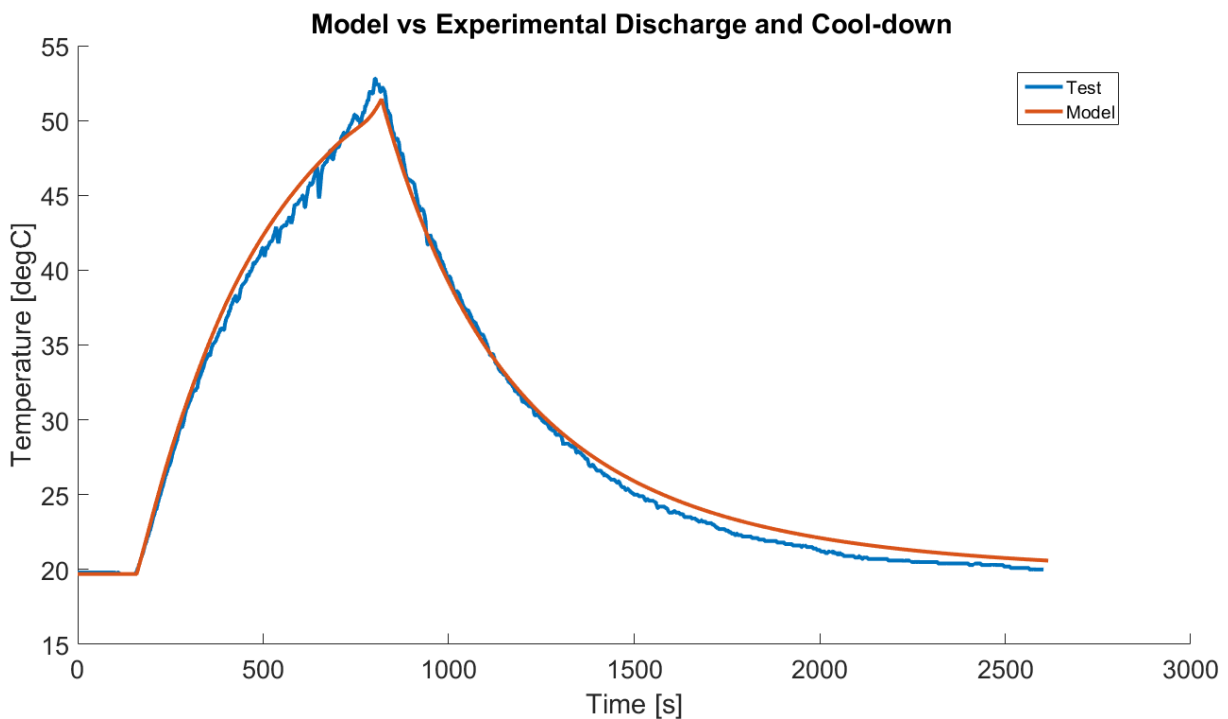


Figure 20: Single pack discharge model vs experimental data.

Full Pack Thermal Model

Once the single cell model was verified and tuned, a full pack model was created to model the temperature behavior of a battery pack consisting of multiple cells. A block diagram of the full pack electrical model is shown in Figure 21. Input parameters such as ambient conditions, current draw, pack state of charge (SOC), and electrical configuration are entered into the model. An electrochemical model then uses these parameters to predict the voltage drop and waste heat generated in each cell of the battery pack. This is then input into a thermal model that computes the heat dissipation out of the cell and, ultimately, the cell temperature.

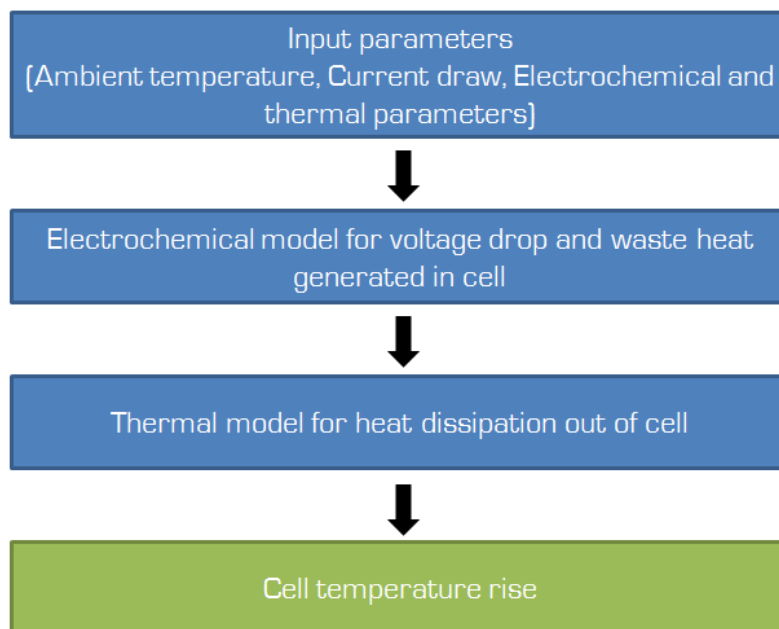


Figure 21: Schematic of full pack thermal model.

To begin the prediction of the battery pack temperature, the geometric and electrical configuration of the cells must be used to determine the heat loss parameters of the pack. Because increasing the parallel string size decreases the current per cell, the number of cells in the pack is important for determining how much power, and thus heat, each cell contributes to the total pack.

The heat stored in the cells and cell temperature rise are governed by this main equation in the model:

$$q_{st} = q_{in} - q_{air} - q_{tab} \quad (13)$$

where q_{air} is the heat lost to convective heat transfer to the air around the pack and q_{tab} is the heat conducted into the bus bars of the cell. A schematic of these heat transfer modes can be found in Figure 22.

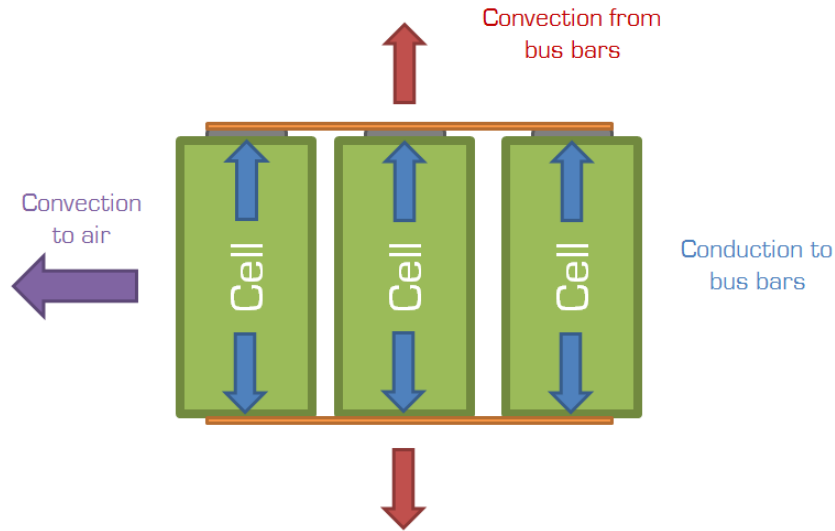


Figure 22: Sources of heat transfer in full pack thermal model.

Like in the single cell thermal model, the heat generated in the cell is modeled using the electrochemical model and the following governing equation:

$$q_{in} = I(OCV - V) \quad (14)$$

The heat lost to the air through convective heat transfer is modeled using:

$$q_{air} = h_{conv}A(T_{cell} - T_{air}) \quad (15)$$

where h_{conv} is the convective heat transfer coefficient of the cell array.

Although the battery pack can be modeled as an array of cylinders in cross-flow, most correlations for heat transfer for such an array assume a fairly large spacing between cylinders to calculate heat transfer coefficients. In battery pack design, however large gaps between the cells are usually an impractical design option. When space is so limited, cells are usually placed very close together (<2mm), making these heat transfer models for arrays of cylinders in cross-flow impractical.

For this reason, to calculate h_{conv} a simplified heat transfer correlation was chosen, representative of a single cylinder immersed in cross-flow [5]:

$$Re = \frac{UD}{\nu} \quad (16)$$

$$Nu = 0.3 + \frac{0.62Re^{1/2}Pr^{1/3}}{\left[1 + \left(\frac{0.4}{Pr}\right)^{2/3}\right]^{1/4}} \left[1 + \left(\frac{Re}{282000}\right)^{5/8}\right]^{4/5} \quad (17)$$

$$h_{conv} = l \frac{(Nu)k}{D} \quad (18)$$

where U is the velocity of the air around the cell, D is the diameter of the cell, ν is the kinematic viscosity of air, Pr is the Prandtl number of air, Re is the Reynolds number, Nu is the Nusselt number, and l is a constant that was tuned to match the measured temperature of the cells measured in the full pack discharge.

When air flows through the pack, the temperature of the air increases as more heat is transferred to it. For this reason, the temperature of the air between the cells was modeled to measure the effects of its increased temperature as it moved through this pack. This was modeled using:

$$0 = q_{air} + \dot{m}c_{air}T_{air_{j-1}} - \dot{m}c_{air}T_{air_j} \quad (19)$$

where \dot{m} is the mass flow rate of air, c_{air} is the specific heat of air, T_{air_j} is the air temperature in the j-th row of cells in the pack.

For each row of cells, air temperature increased as the air passed through the pack. With the increased temperature in air, properties such as air density, Prandtl number, viscosity, and thermal conductivity changed. Thus for each row of cells, a new heat transfer coefficient was calculated to capture the effects of the temperature rise.

To model the pack's heat transfer to the bus bars, the following equation was used:

$$q_{tab} = \frac{(T_{cell} - T_{bar})}{R} \quad (20)$$

where R is the thermal resistance of the bus bar. Unlike in the single cell discharge, where a large heat sink electrode was affixed to the cell, in a full pack scenario, usually bus bars are affixed to the cell using a few small spot welds or laser welds. Because the contact area of these welds is much smaller, the contact pressure is much lower, and the bus bars are much thinner in a full pack versus a single cell discharge setup, there is less heat transfer to the bus bars in the full pack. For this reason, thermal resistance of the bus bar is fairly high and much less heat gets transferred from the cell by this mode than in the single cell discharge.

Since the thermal resistance of the bus bar is relatively high and the bus bar material has high thermal conductivity, a lumped thermal mass model was used to predict the bus bar temperature. The model accounts for the number of bus bars and their physical properties (surface area, cross-sectional area, material), and the temperature is calculated assuming that all bus bars are lumped together into a single thermal mass. The temperature is then predicted by:

$$m_{bar}c_{bar}\frac{dT_{bar}}{dt} = q_{tab} - h_0A(T_{bar} - T_{air}) \quad (21)$$

where m_{bar} is the mass of the bus bars, c_{bar} is the specific heat capacity of the bus bar, T_{bar} is the temperature of the bus bar, h_0 is the natural convection heat transfer coefficient for the bus bar, A is the surface area of the bus bar, and T_{air} is the temperature of the air around the bus bar assembly.

When tuning the full pack model, good correlation to experimental data of air temperature rise inside the pack as well as bus bar temperature rise was achieved, as illustrated in Figure 23. It can be noted that after 350 seconds, the pack is no longer being discharged and starts to cool.

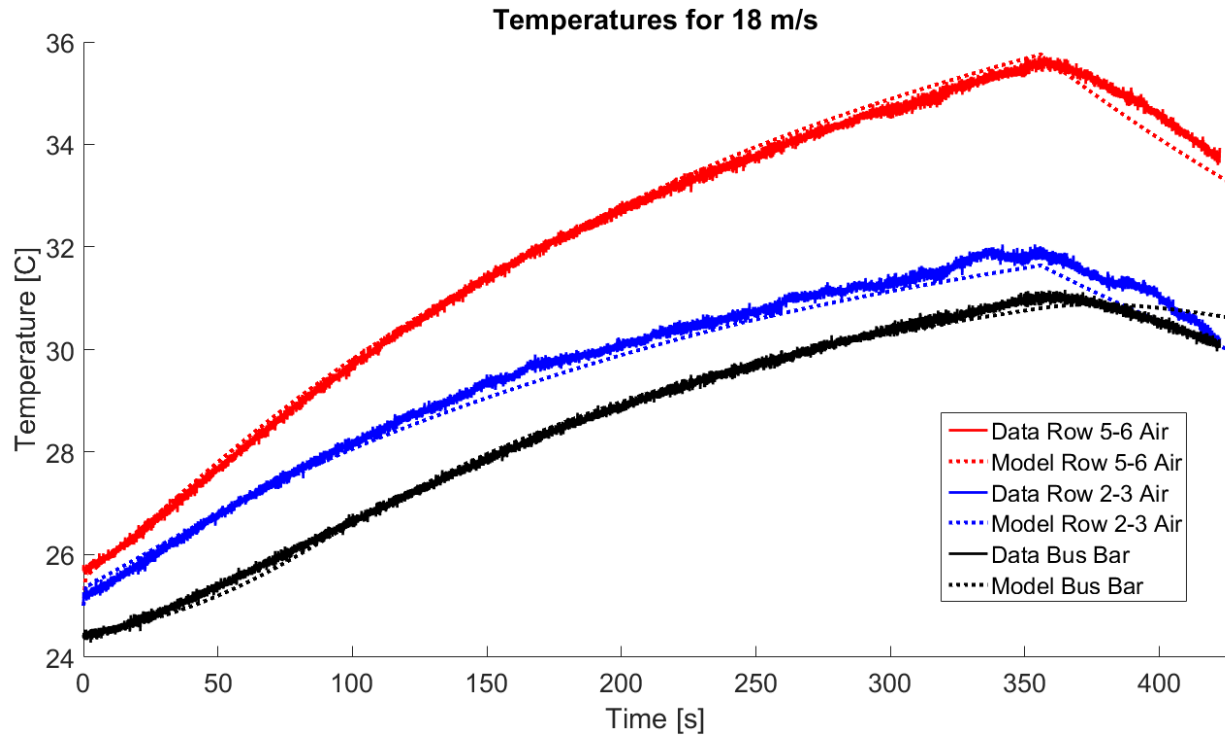


Figure 23: Full pack experimental data vs model at 18 m/s inlet air speed.

This led to a prediction of individual cell temperatures throughout the pack, as seen in Figure 24. It can be noted that the model predicts that with each cell row's increased distance from the air inlet, cell temperature increases. This is due to the increased air inlet temperature for each row of cells as the air heats up moving through the pack.

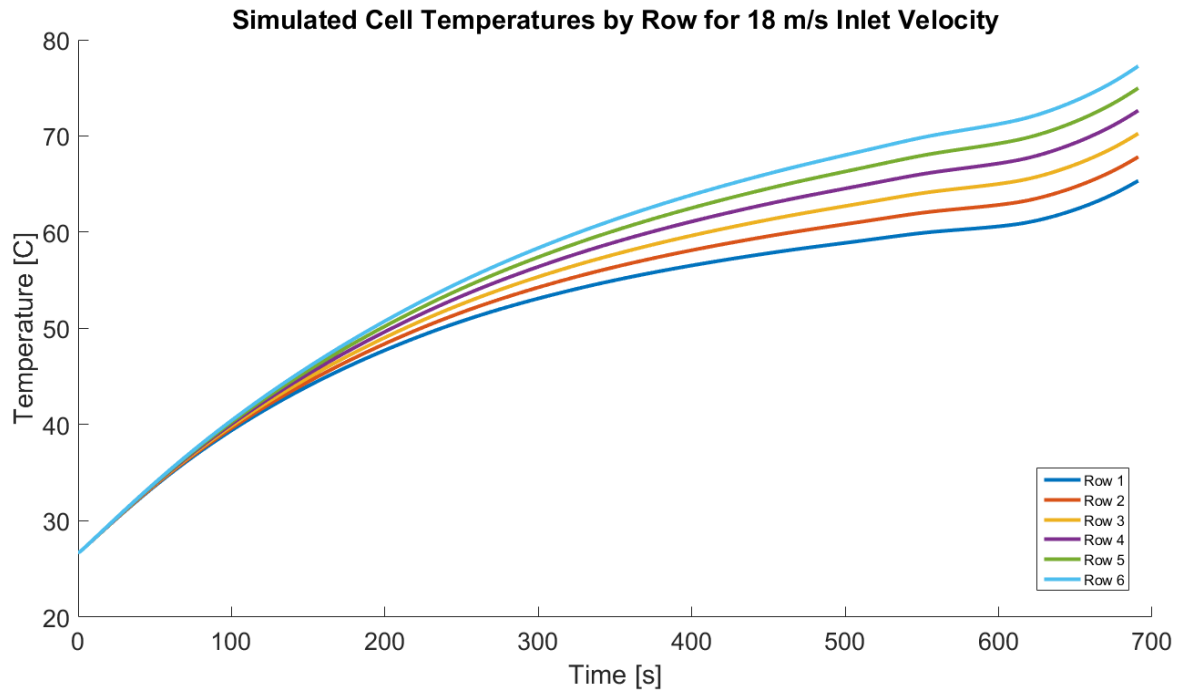


Figure 24: Predicted cell temperatures in prototype pack.

Next, a GUI was developed for this full pack model, so that users may easily iterate between different pack parameters when performing simulations and design of experiments (Figure 25).

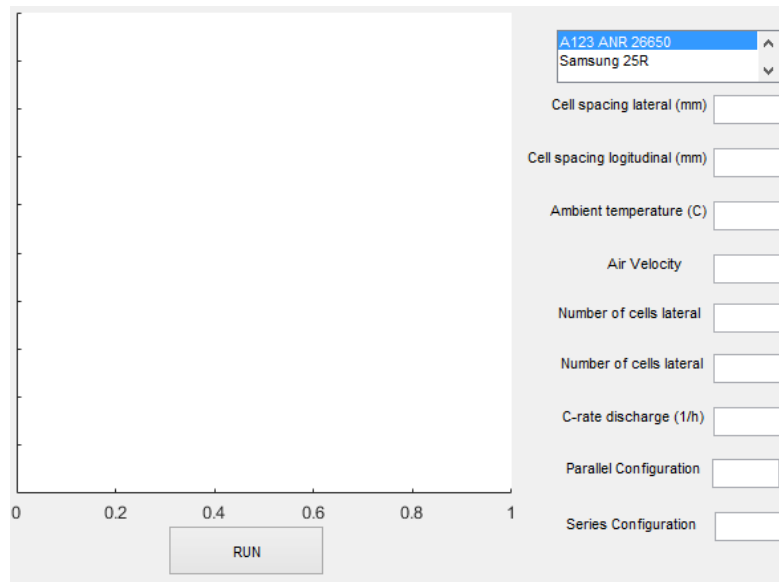


Figure 25: Model GUI.

Chapter 5: Case Studies

Because this developed model is useful in predictive comparisons between different pack design parameters, it is useful in answering some of the questions in pack design regarding the effects of changing configuration of the pack.

Effects of cell spacing

One of the major difficulties in designing air cooled cylindrical cell packs is determining the spacing required between the cells in order to achieve proper cooling. The model for full pack temperature predicts that with larger gaps between the cells, there is less temperature rise in each cell (Figure 26).

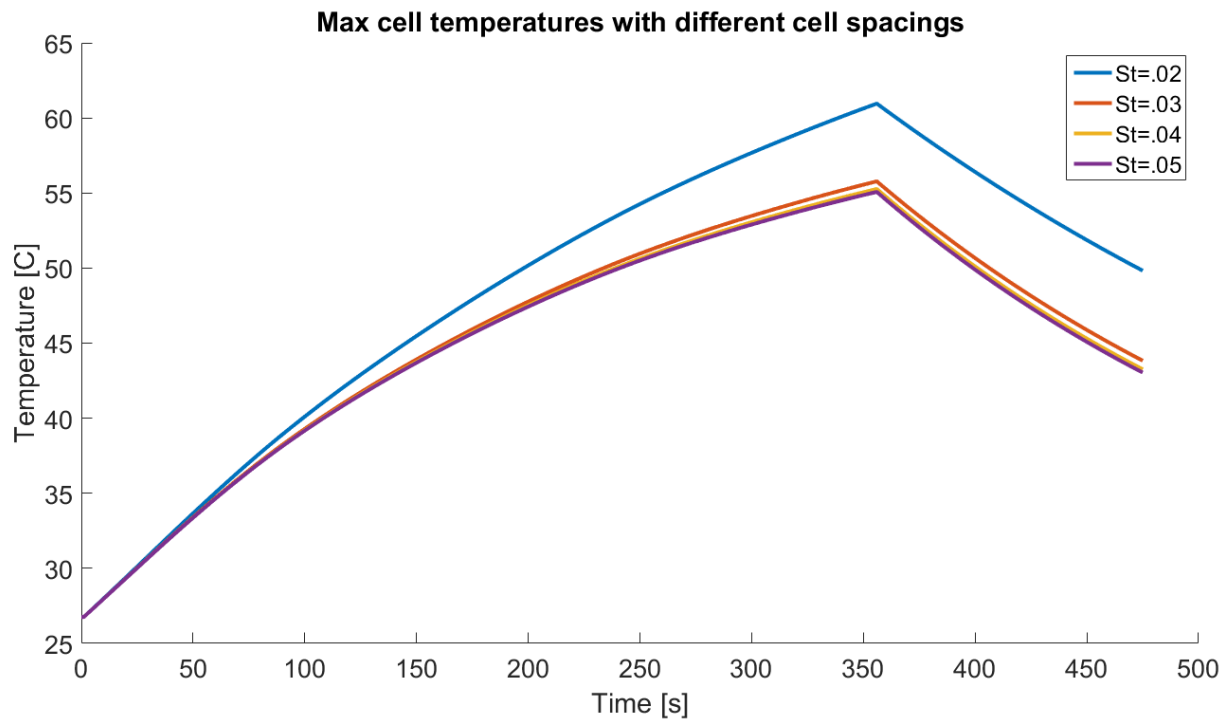


Figure 26: Temperature profiles at different cell spacing.

It can be noted, however, that the relationship between the cell temperature and cell spacing is not linear. The temperature decreases with cell spacing but asymptotically approaches a limit, as shown in

Figure 27. This is due to the dependence on spacing in the mass flow rate of the air passing through the battery pack.

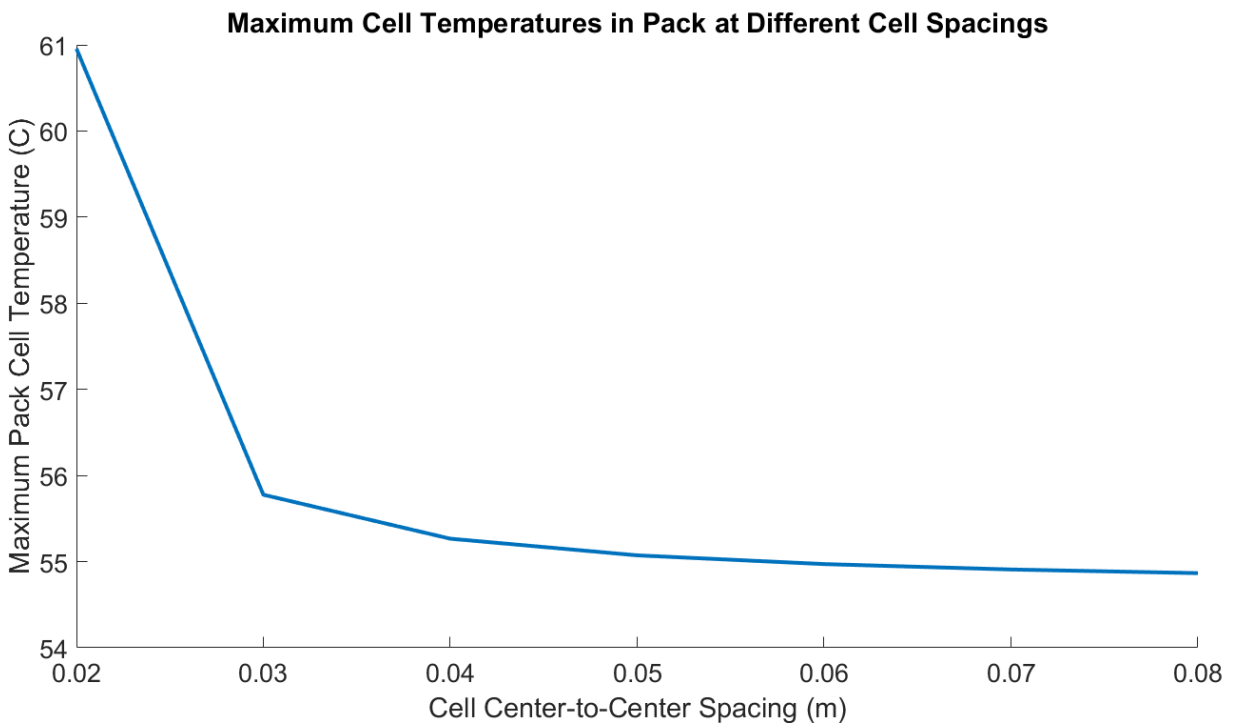


Figure 27: Spacing effect on cell temperature.

Effects of Air Speeds

With active air cooling systems it is important to understand which air velocities are required to meet cooling requirements of the battery pack. In passive cooling systems relying solely on the speed of the vehicle to cool the battery pack, understanding the effect of vehicle speed on cell temperature in the battery pack. Figure 28 shows the relationship between inlet air velocity and cell temperature.

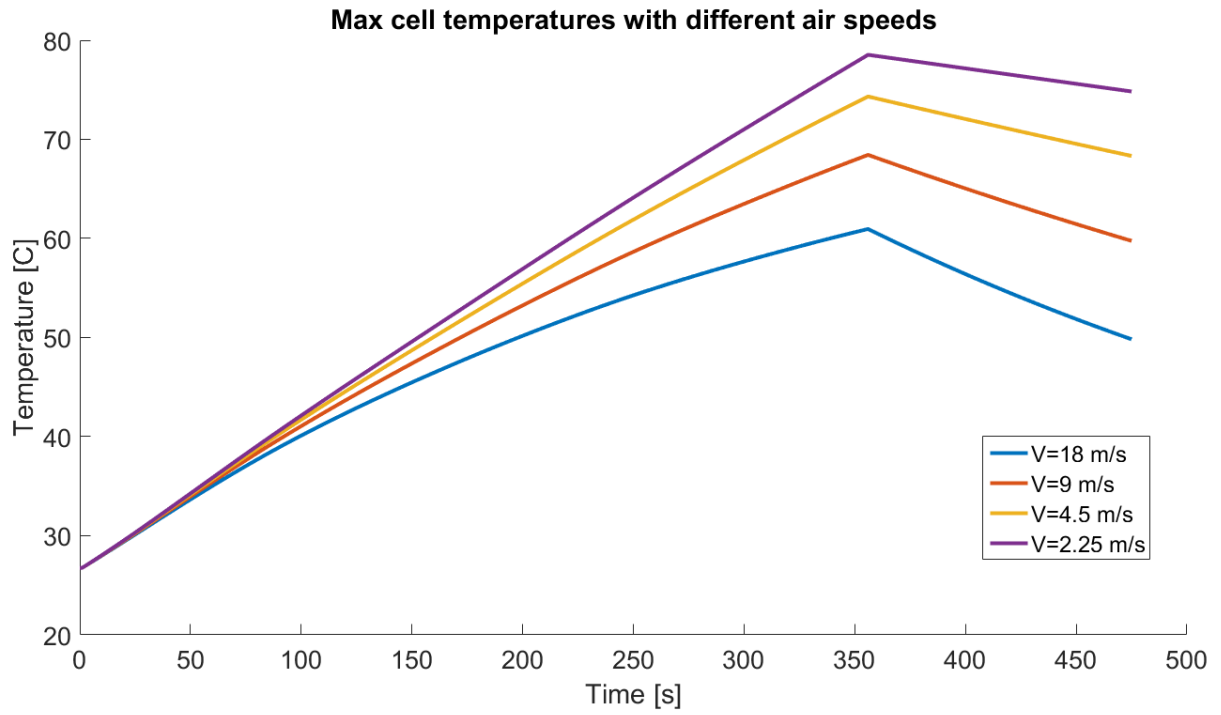


Figure 28 Temperature profiles at different air inlet velocities.

Figure 29 further portrays the relationship between air inlet velocity and cell temperature in the full pack model.

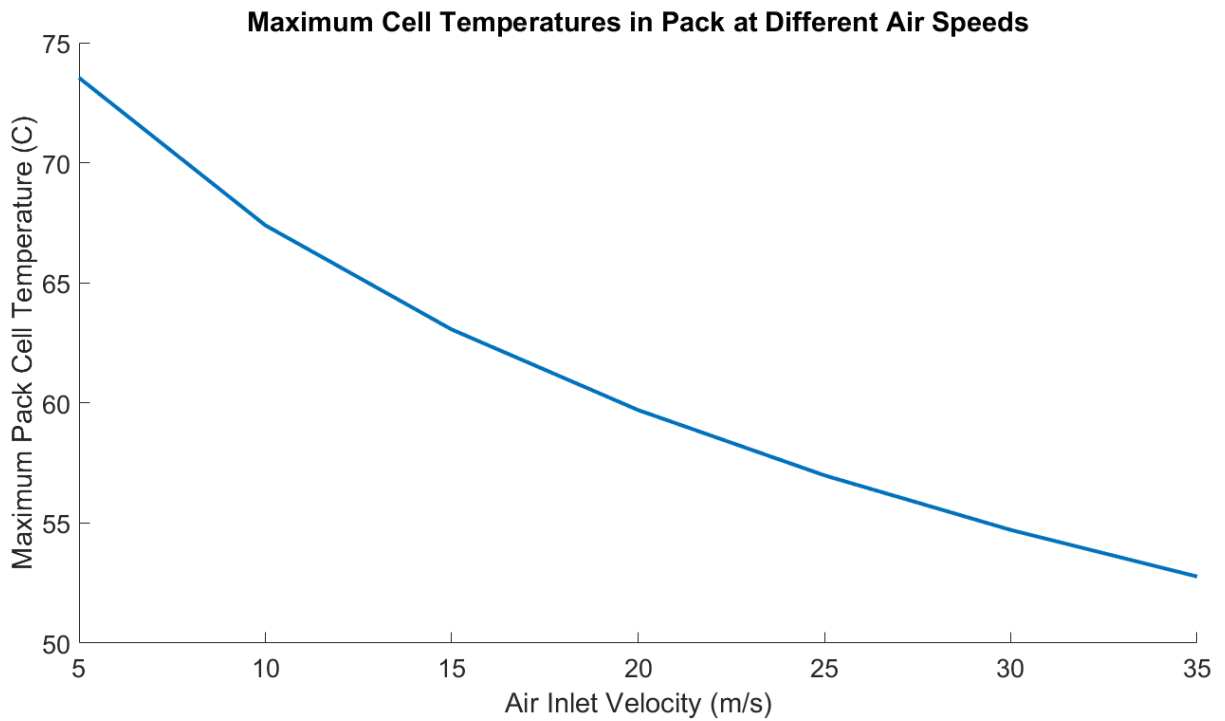


Figure 29: Air velocity effect on cell temperature

Effects of Cell Chemistry

The model can also be used to study the comparative thermal behavior between different cell chemistries. When the Samsung 25R NCA battery cell used in RW-3 is compared to the A123 ANR26650 LiFePO_4 battery that Buckeye Current plans on using on their 2016 motorcycle, it is clear that the A123 cell performs much better from a thermal standpoint (Figure 30). This is due to its much higher power density and continuous current discharge capabilities.

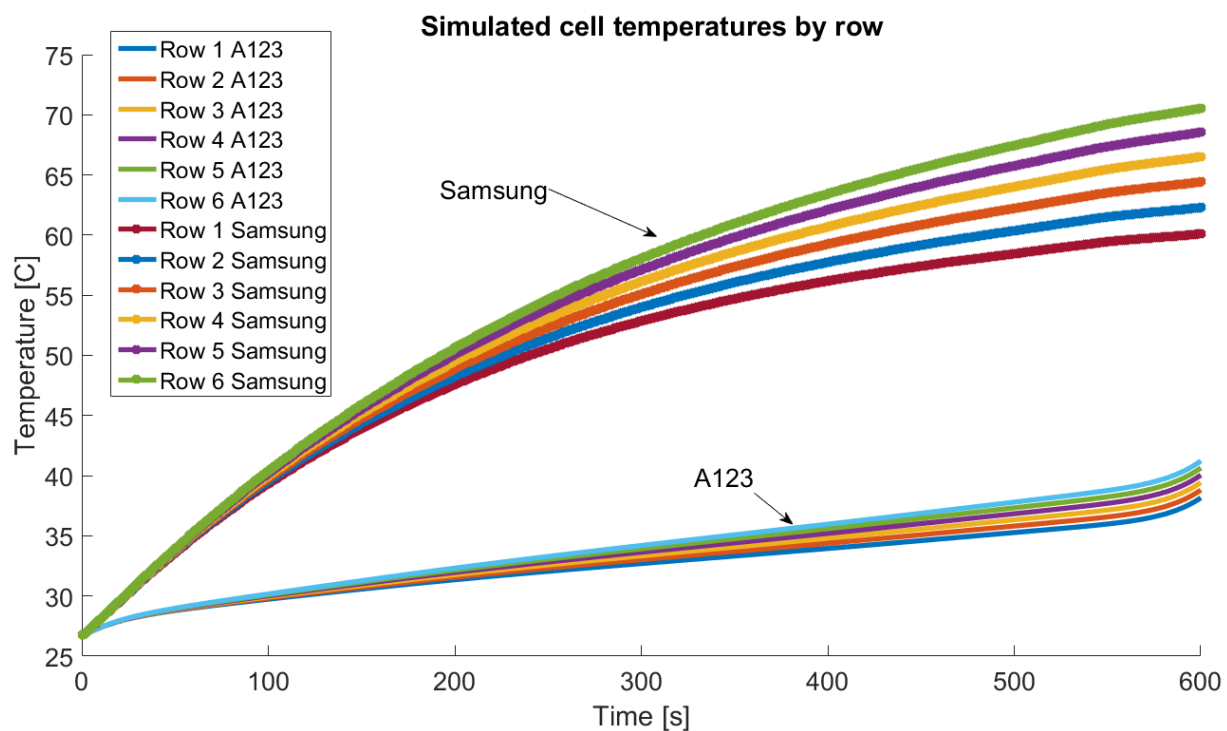


Figure 30: A123 vs Samsung predicted thermal performance.

It can be noted that although the A123 cell maintains a lower temperature than the Samsung cell during discharge, the cells have very different energy and power densities (as shown in Table 1 below). These variables should be considered alongside the thermal performance when designing a battery pack, since there are usually stringent weight and volume requirements in a vehicle battery pack build.

Table 1: Comparison of Samsung and A123 power and energy densities.

Cell Parameter	Samsung 25R	A123 ANR26650
Chemistry	NCA	LiFePO ₄
Gravimetric Power Density (W/kg)	2000	3080
Volumetric Power Density (W/L)	5441	6695
Gravimetric Energy Density (Wh/kg)	209	110
Volumetric Energy Density (Wh/L)	544	239

Parallel Configuration

Another variable that battery pack designers often deal with is the electrical configuration of the battery pack. While series configuration is usually limited by system voltage requirements, adding more parallel strings to a pack is a way to decrease the current draw from each individual cell while adding more thermal mass (more cells) to the system. Figure 31 illustrates a battery pack made of Samsung 25R cells with different parallel string configurations being discharged at a continuous 30A. Using the full pack thermal model, it is evident that adding parallel cells can be an effective method in reducing temperature rise in the pack. However, the benefits tend to significantly reduce after 4 parallel strings, indicating a trade-off between pack design and thermal performance.

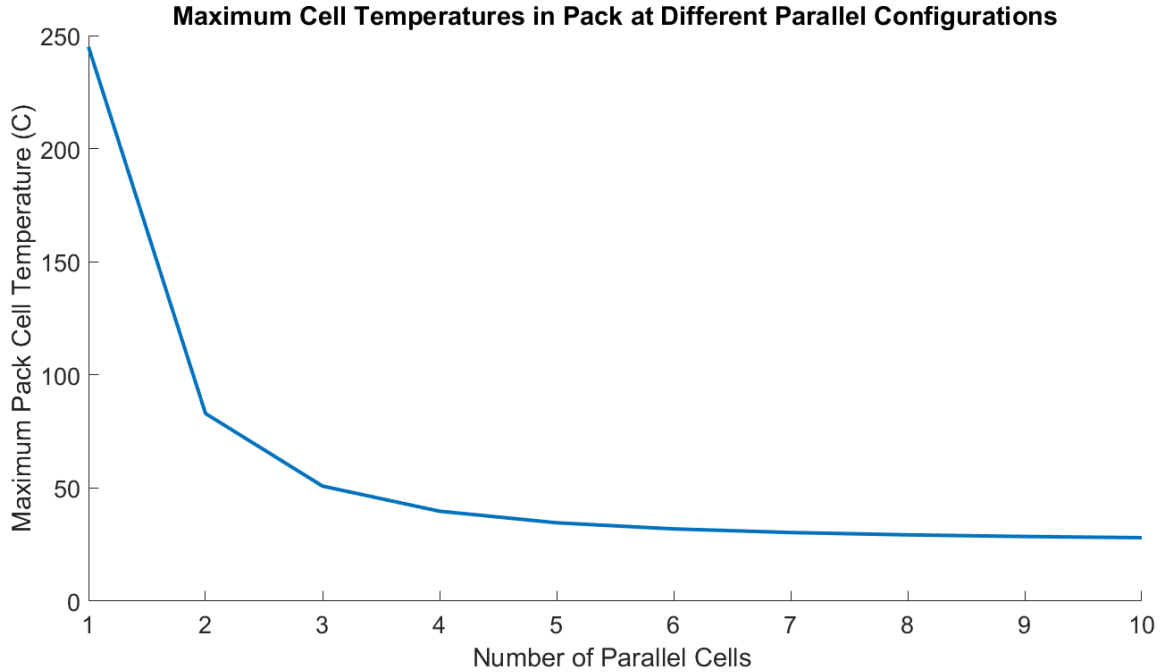


Figure 31: Parallel string configuration effect on cell temperature.

Chapter 6: Conclusion/ Recommendation for future work

In this study, an electrochemical model for two different cell chemistries was developed and used to create a single cell and full pack temperature predictive model for cylindrical Li-ion batteries. The resultant models are useful tools for comparative design studies between different battery pack parameters. It lets design engineers iterate parameters such as air velocity, cell chemistry, electrical configuration, and cell spacing to see the effects on the thermal performance on a battery pack. This makes the model a useful tool for pack design.

Future work includes verifying the model with more battery packs to ensure predictive correlations are accurate. More verification of the model is required in the future, particularly in more complex and dynamic air velocity and battery pack current conditions. Predictive capability for dynamic loading on the cell is a useful tool, especially on Buckeye Current's PPIHC motorcycles where there is a wide range of

vehicle velocities, changing ambient conditions on the mountain course, varying air speeds over different parts of the battery pack, and constant pulses of peak current. Further development in these more complex multifarious conditions would be useful for capturing more of the complex behavior occurring in battery packs on-board vehicles.

The model can be further developed with more test data and eventually capture cell temperature behavior well enough to not only be used as a design tool, but also as an on-board predictive tool.

Buckeye Current plans on instrumenting the battery pack on its 2016 vehicle RW-3x (shown in Figure 32 and Figure 33) with temperature sensors in order to continue the development of this model. The data from the next race bike battery pack will be useful for the future development of the model and will continue to improve the work of this study.

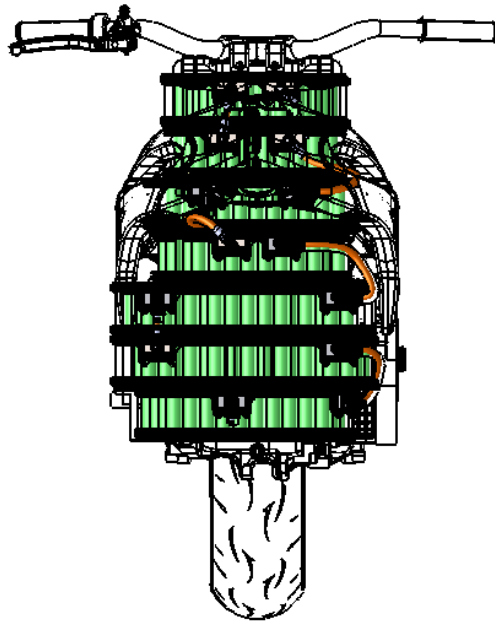


Figure 32: PPIHC 2016 battery pack placement in vehicle.

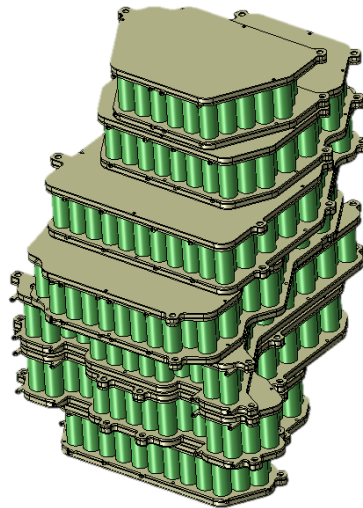


Figure 33: RW-3x battery pack isometric view.

References

- [1] PPIHC. (n.d.). Retrieved March 17, 2016, from <http://www.ppihc.com/>
- [2] Christopher D. Rahn and Chao-Yang Wang, "Battery System Engineering," A John Wiley & Sons, Ltd., Publication (2013).
- [3] Marcicki, J., Canova, M., Conlisk, A. T., & Rizzoni, G. (2013). Design and parametrization analysis of a reduced-order electrochemical model of graphite/LiFePO₄ cells for SOC/SOH estimation. *Journal of Power Sources*, 237, 310-32
- [4] Fan, G., Pan, K., Bartlett, A., Canova, M., & Rizzoni, G. (2014, October). Electrochemical-Thermal Modeling of Li-Ion Battery Packs. In *ASME 2014 Dynamic Systems and Control Conference* (pp. V002T23A004-V002T23A004). American Society of Mechanical Engineers.
- [5] Incropera, F. P. (2007). *Fundamentals of heat and mass transfer*. Hoboken, NJ: John Wiley.
- [6] Smith, Kandler, and Chao-Yang Wang. "Power and thermal characterization of a lithium-ion battery pack for hybrid-electric vehicles." *Journal of power sources* 160.1 (2006): 662-673.
- [7] Fang, Weifeng, Ou Jung Kwon, and Chao-Yang Wang. "Electrochemical-thermal modeling of automotive Li-ion batteries and experimental validation using a three-electrode cell." *International journal of energy research* 34.2 (2010): 107-115.

[8] Guo, Meng, and Ralph E. White. "A distributed thermal model for a Li-ion electrode plate pair." *Journal of Power Sources* 221 (2013): 334-344.

Appendix A: Parameter Values Used in Thermal Models

Table 2: Parameters used in single cell thermal model (Samsung 25R)

Parameter	Value	Units
Cell mass, m	45	g
Cell specific heat capacity, c_{cell}	0.974	J/kg-K
Ambient temperature, T	19.7	°C
Length of cell, L	0.065	m
Diameter of cell, D	0.018	m
Air specific heat, c_p	1007	J/kg-K
Coefficient of thermal expansion of air, B	0.0034	1/K
Dynamic viscosity of air, ν	0.0000185	kg/m-s
Air density, ρ	1.201	Kg/m ³
Thermal conductivity of air, k	0.0261	W/m-K
Emissivity	0.85	-
Prandtl number for air, Pr	0.7138	-
Fraction of heat not dissipated through cell tabs, c	0.6	-

Table 3: Parameters used in full pack thermal model of test pack

Parameter	Value	Units
Parallel string, p	3	cells
Series string, s	8	cells
Width of pack studied, w	4	cells
Depth of pack studied, d	6	cells
Cell mass, m	45	g
Cell specific heat capacity, c_{cell}	0.974	J/kg-K
Ambient temperature, T	26	°C
Length of cell, L	0.065	m
Diameter of cell, D	0.018	m
Length of bus bar, l_{bar}	0.02	m
Width of bus bar, w_{bar}	0.06	m
Depth of bus bar, d_{bar}	0.000254	m
Number of bus bars, n_{bars}	10	-
Density of bus bar (nickel 200 material), ρ_{bar}	8890	kg/m ³
Thermal resistance of bus bar connection, R	180	K/W
Bus bar specific heat capacity, c_{bar}	0.456	J/kg-K

* Note that in the full pack model, physical properties of air were obtained from a look-up table based on calculated air temperature. [5]